

ON THE EFFECTIVENESS OF CLASSICAL REGRESSION METHODS FOR OPTIMAL SWITCHING PROBLEMS

MARTIN ANDERSSON, BENNY AVELIN, AND MARCUS OLOFSSON

ABSTRACT. Simple regression methods provide robust, near-optimal solutions for optimal switching problems in dimensions ranging from 1 to 50. While the theory requires solving intractable PDE systems, the Longstaff-Schwartz algorithm with classical approaches like k -NN achieves excellent switching decisions without extensive hyperparameter tuning. Testing eight regression approaches on four benchmark problems, we find that simple methods maintain stable performance across diverse problem characteristics, even after extensive neural network optimization. The contaminated training targets inherent to backward induction—where each target contains both approximation bias and Monte Carlo noise—actually favor these robust approaches over more complex alternatives such as neural networks. Further, we establish concentration bounds for k -NN regression under jump-diffusion dynamics and show that PCA enables k -NN to scale to high dimensions. For practitioners: simple, minimally-tuned regression methods offer reliable performance for computationally demanding switching problems.

CONTENTS

1. Introduction	1
2. Literature overview	2
3. Setup of the problem	4
4. Regression models for optimal switching	7
5. Theoretical guarantees for the Longstaff-Schwartz algorithm	9
6. Numerical experiments	12
7. Results of numerical experiments	17
8. Discussion and conclusion	17
Acknowledgments	22
References	22
Appendix A. Additional tables	26
Appendix B. Implementation Details	28
Appendix C. Proof of Theorem 5.3	29
Appendix D. Proof of Theorem 5.4	33
Appendix E. Jump diffusion processes and verification of (5.6)	35

1. INTRODUCTION

Managers of complex production systems face a challenging problem: how to decide when to switch between different operational modes when facing uncertain market conditions and significant switching costs? This question arises across industries, from energy production choosing between different fuel sources to manufacturing plants shifting between different product lines. The mathematical framework of *Optimal Switching* (OS) provides a principled approach to these decisions, yet a significant gap exists between theoretical solutions and practical implementation. These switching decisions carry substantial economic weight. In energy markets, the difference between optimal and suboptimal switching can represent a substantial loss in annual revenue. A poorly-timed switch can lock a facility into an inefficient mode just as conditions shift, while excessive switching erodes profits through transition costs.

While the mathematical foundations of OS are well-established through solutions to systems of parabolic PDEs with interconnected obstacles, these theoretical solutions remain computationally intractable for realistic problems. These PDE systems are difficult to manage even numerically, and without explicit solutions we cannot construct switching strategies to support actual decision-making. Consider a manager facing a just 10-dimensional state space, (comprised of multiple correlated fuel costs, energy prices, weather conditions and forecasts). Traditional finite differences with just 100 grid points in each dimension would require 10^{20} points to solve for, exceeding any current computational abilities.

A classical approach to similar problems, particularly in the context of American options, involves simulation and regression methods, see the seminal papers [LS01] and [TVR99]. These involve simulating data and then using dynamic programming principles, recursively defining the problem, and iteratively applying regression methods. These methods shift the computational burden from solving high-dimensional PDEs to a statistical estimation problem: given simulated paths of the underlying stochastic factors, can we learn the continuation values needed for optimal decisions? This approach faces its own dimensional challenges but offers more flexibility in addressing them. While this approach has been studied extensively in option pricing, its effectiveness in the more complex OS setting with multiple sequential decisions rather than a single exercise time is underexplored, both theoretically and practically.

Given the complexity of OS problems, one might expect that sophisticated machine learning methods, particularly deep neural networks, would be necessary for optimal performance. Our findings challenge this intuition. Through a combination of new theoretical analysis and comprehensive experiments, we demonstrate that classical methods, in particular k -nearest neighbor regression, can match or exceed the performance of complex alternatives while maintaining stable decision boundaries, requiring minimal hyperparameter tuning, and offering computational efficiency.

Our contributions in this paper are the following:

- **Theoretical guarantees:** We establish error bounds on regression with k -NN regression in the Longstaff-Schwartz algorithm under both diffusion and jump-diffusion dynamics, covering subgaussian and subexponential tails (Section 5)
- **Comprehensive empirical comparison:** We comprehensively compare a range of parametric and non-parametric regression models, ranging from linear models to neural networks, on a suite of management problems from the OS literature, including high-dimensional (~ 50) ones (Section 6).
- **Simple methods excel:** We find that very simple models, like k -NN, can achieve almost optimal management decisions, including in high dimensions, when paired with straight-forward dimensionality reduction such as Principal Component Analysis (PCA) (Section 7)

2. LITERATURE OVERVIEW

The mathematical theory of OS is well studied and contributions have been made from a long list of researchers. Without any aspiration to give a complete list, contributions can be found in, e.g., [BGSS22, BJK10, DHP09, EAF17, EAH09, HM13, HT10, Kha16, LNO14a, LNO14b, LO22, Mar16, Per18, Per20, Per21]. On a more fundamental level, the concepts of backward stochastic differential equations and viscosity solutions for PDEs are of critical importance for the development of OS theory, and we refer to [CIL92, PP90, PP92] for introductions to these concepts. As the standard setting has been understood, many alternative formulations of the OS have been considered, e.g., game settings [HMM19], delayed decisions and memory [Per18, Per20], partial information [LNO15, Olo18], state constraints [Kha16], and numerical methods based on simulations [ACLP14, LOO21].

When it comes to applications, the literature is far less developed. This contrasts to what could be expected given the importance of closely related topics in financial mathematics; see, e.g., [EKPQ97], and [PS06] for an overview. Typically, the applications considered are

low-dimensional and rather unrealistic from a practitioner point of view; see, e.g., [BØ94, BS85]. A literature survey indicates that, besides [ACLP14, CL08, CL10, LOO21] concrete applications of optimal switching in at least semi-realistic settings are hard to come by.

A major challenge in the quest for explicit value functions of OS problems is the quickly increasing dimensionality of the problem when applied to more realistic settings. This dimensionality becomes an issue as most numerical methods suffer heavily from the “curse of dimensionality”. Starting with [Ti93], a classical approach to overcoming this difficulty in option pricing is to ignore the connection to PDEs and instead exploit the stochastic formulation of the optimization problem as an expected value of some functional of a stochastic process; the value function can then be found using Monte Carlo methods. Several attempts have been made to improve this idea using regression, some of the most well-known attempts being [BG97, Car96, HK04, LS01, Rog02, TVR99]. There have been a few efforts to apply more general regression methods to the problem; see [CL08, ACLP14, BCN23], but the literature is scarce.

Regarding machine learning and neural networks (NNs) for stochastic control problems, attempts were made already a decade ago to study the optimal stopping problem using a NN with a single hidden layer, see [KKT10]. Recently, much attention has been directed to this problem from researchers in various fields, including mathematics, finance, data science, and physics. In particular, the closely related case of optimal stopping has been extensively studied during the last years; see, e.g., [BCJ19, BCJ21, BHRS23, EM21, FD21, Hu20, HKRT24].

There has also been significant effort devoted to using NNs to solve high dimensional PDEs associated with stochastic control, notably the seminal papers [HJW18, HPW19]. This has also been extended to jump diffusions in [GPP22]. These ideas were later used in [BCN23] to solve OS problems using neural networks. The theoretical foundations for these neural network approaches rely on universal approximation theorems [HSW89, Cyb89] which establish that neural networks can approximate any continuous function on compact sets to any given precision, given sufficient width or depth. Later, the capabilities of these networks have been enhanced through advances in architecture design [BGC17], and optimization techniques [KB14].

Several classical machine learning approaches also offer promising capabilities for addressing high-dimensional OS problems, potentially mitigating the curse of dimensionality. Random forests [Bre01] implicitly perform feature selection through random subspace sampling and provide built-in variable importance measures, making them effective for identifying relevant features in high-dimensional spaces. Similarly, boosted tree methods [Fri01] sequentially build models that focus on errors from previous iterations, naturally emphasizing informative features. Further, histogram approaches [KMF⁺17] make these models highly efficient in high dimensions. For linear approaches, LASSO regression [Tib96] induces sparsity through L1 regularization, effectively performing automatic feature selection by shrinking irrelevant coefficients to zero. Ridge regression [HK70] employs L2 regularization to stabilize estimation in the presence of multicollinearity, which frequently occurs in high-dimensional financial and economic time series. Even simple non-parametric methods like k -nearest neighbors [CH67], when combined with appropriate dimensionality reduction techniques, can use detailed local structure in the state space without imposing restrictive functional form assumptions. These methods offer varying trade-offs between interpretability, computational efficiency, and flexibility in high dimensions that may prove advantageous for OS problems compared to more complex deep learning approaches.

The theoretical advantages of these classical methods align with empirical findings in the machine learning literature, which documents numerous instances where they outperform neural network approaches. For example, a comprehensive study of real-world classification tasks [FDCBA14] demonstrated that random-forests were most likely to achieve top performance against various classifiers, including NNs. In time series forecasting, [ETR⁺21] showed that with appropriate pre-processing, simpler gradient-boosted trees [Fri01] can outperform neural networks. Further, [SWL⁺16] showed for high-dimensional (> 1000) regression tasks in chemical modeling, gradient boosting achieve almost on-par performance with deep neural nets, with a

fraction of the computational burden. Similarly, a systematic analysis [FDCJ19] of algorithm proposals for top-n recommendation tasks, showed nearest-neighbor based systems surpassed more complex neural network systems. Notably, in the specific context of OS problems, no comprehensive comparison between neural network approaches and more classical machine learning methods has been conducted to our knowledge—a gap our present work aims to address.

3. SETUP OF THE PROBLEM

3.1. The general challenge of optimal switching. Optimal switching problems with realistic multidimensional state processes resist analytical solution. When the underlying process X_t involves multiple correlated market variables, the curse of dimensionality makes standard finite difference PDE methods computationally infeasible.

A more viable solution is to use Monte Carlo regression methods like Longstaff-Schwartz [LS01], but these introduce three major challenges. First, each regression step produces contaminated training targets. Unlike standard supervised learning where true training labels are observed, optimal switching requires estimating value functions that depend on future value functions that are themselves approximated. This nested structure propagates and amplifies approximation errors through the backward induction.

Second, the method requires training $N \times D$ separate regression models (one for each time step and production mode). With typical problems involving hundreds of time steps and multiple modes, computational scaling becomes a dominant constraint on method selection.

Third, each individual regression model must be able to handle high-dimensional feature spaces. Many applications can involve 10–50 market variables (electricity prices across regions, multiple fuel costs, weather patterns, demand forecasts), creating feature spaces where many methods suffer from the curse of dimensionality or require prohibitively large training datasets.

3.2. Production facility setup. Consider a production facility operating in D modes under random market conditions $X_t \in \mathbb{R}^d$. Let X_t be a continuous-time Markov process representing market conditions (electricity prices, fuel costs, weather). Each production mode $i = 1, \dots, D$ generates instantaneous payoff $f_i(x, t)$ in state x at time t , with switching costs $c_{ij}(x, t)$ between modes.

A production strategy is a random function $\mu(t)$ indicating the active production mode at time t , adapted to the process X_t . This corresponds to a sequence of (stopping) switching times $\{\tau_k\}$ and modes $\{\xi_k\}$ (post-switch modes):

$$\mu(t) = \xi_k \quad \text{for } \tau_k \leq t < \tau_{k+1}. \quad (3.1)$$

3.3. Mathematical formulation. The total expected payoff for a given strategy μ starting in mode i at time t and state x is:

$$J_i(t, x, \mu) = \mathbb{E} \left[\int_t^T f_{\mu(s)}(s, X_s) ds - \sum_{T \geq \tau_k > t} c_{\xi_{k-1}, \xi_k}(\tau_k, X_{\tau_k}) \middle| X_t = x \right]. \quad (3.2)$$

The value function is the supremum over all admissible strategies:

$$V_i(t, x) = \sup_{\mu} J_i(t, x, \mu). \quad (3.3)$$

It is a classical result of OS that, under rather weak conditions (see for instance [TY93]), this value function solves the following system of PDEs

$$\begin{aligned} \min\{-\partial_t V_i - \mathcal{L}V_i - f_i, V_i - \max_{j \neq i}\{V_j - c_{ij}\}\} &= 0, \\ V_i(T, x) &= 0, \end{aligned} \quad (3.4)$$

where \mathcal{L} is the infinitesimal generator of the process X_t .

Once one has access to the value functions $V_i(t, x)$, the optimal strategy can be found by following the optimal switching times. The optimal decision when in mode i is to switch to mode \hat{j} as soon as the process $V_i(X_t)$ hits its obstacle $\max_{j \neq i} \{V_j - c_{ij}\}$, i.e., the first time τ such that

$$V_i(\tau, X_\tau) \leq \max_{j \neq i} \{V_j(\tau, X_\tau) - c_{ij}(\tau, X_\tau)\}, \quad (3.5)$$

and $\hat{j} = \arg \max_{j \neq i} \{V_j(\tau, X_\tau) - c_{ij}(\tau, X_\tau)\}$.

3.4. Numerical solution approach. In this section we detail the Longstaff-Schwartz approach we use in this paper.

3.4.1. Process and discretization. The underlying market process follows jump-diffusion dynamics, where jumps capture sudden market disruptions from weather events, plant outages, or demand spikes:

$$dX_t = \mu(s, X_s) dt + \sigma(s, X_s) dW_s + \gamma(s, X_s) dJ_t, \quad (3.6)$$

where $\mu(s, x)$ is a drift term, $\sigma(s, x)$ is a diffusion term, γ are the jump sizes and J_t is a jump process, dW_t is a d dimensional Brownian motion. In our experiments γ will be a diagonal matrix and each component of J_t will have the form

$$J_t^i = \sum_{j=1}^{\infty} Y_j^i \mathbb{I}_{\{T_j^i \leq t\}}, \quad (3.7)$$

where T_j^i is the time of the j -th jump of the i -th component of the process. The jump process J_t is assumed to be independent of the Brownian motion and the jump times are assumed to be independent of each other.

We discretize the time $[0, T]$ under consideration into $\mathcal{T} = \{0 = t_0, t_1, \dots, t_N = T\}$ with $\Delta t = T/N$ and only allow mode switching at these times, reflecting operational constraints in real production facilities. The continuous part of the paths X_{t_n} , $n = 0, \dots, N$, are simulated according to the standard Euler-Maruyama scheme, and at each time step, we simulate the number of jumps and add their cumulative impact to the diffusion update.

Now let μ be a (discrete) management strategy with switching times $\tau_0, \tau_1, \dots, \tau_{N-1}$. The (discretized) expected profit using μ from $t = t_n$ to $T = t_N$ is then (denoting it again with J_i)

$$J_i(t_n, x, \mu) = \mathbb{E} \left[\sum_{k=n}^{N-1} \Delta t f_{\mu_k}(t_k, X_{t_k}) - \sum_{\tau_k \geq t} c_{\xi_{k-1} \xi_k}(\tau_k, X_{\tau_k}) \middle| X_n = x, \xi_0 = i \right],$$

and the (discretized) value function is defined by (denoting it again with V_i)

$$V_i(t_n, x) = \max_{\mu} J_i(t_n, x, \tilde{\mu}). \quad (3.8)$$

3.4.2. The Regression Problem. The value function satisfies a dynamic programming relation:

$$V_i(t_n, x) = \mathbb{E} \left[\max_j [\Delta t f_j(t_n, X_{t_n}) - c_{ij}(t_n, X_{t_n}) + V_j(t_{n+1}, X_{t_{n+1}})] \middle| X_n = x \right]. \quad (3.9)$$

The Longstaff-Schwartz algorithm estimates this conditional expectation using regression, but faces the fundamental challenge that future value functions $V_j(t_{n+1}, \cdot)$ are unknown. We can only use approximations $\hat{V}_j(t_{n+1}, \cdot)$ from previous time steps, contaminating every training target with both systematic bias from previous approximations and Monte Carlo noise.

To set up our approach, we first let $D_T = \{X_{t_0}^i, \dots, X_{t_N}^i; i = 1, \dots, M\}$ be the set of all states at all times for $M \in \mathbb{N}$ independent trajectories defined in the previous subsection. The processes starting points are drawn from a distribution μ_0 which is assumed to be sub-Gaussian, see Definition C.2.

The targets we estimate at each time-step are:

$$\tilde{V}_i(t_n, x) = \mathbb{E} \left[\max_j (\Delta t f_j(x, t_n) - c_{ij}(x, t_n) + \hat{V}_j(t_{n+1}, \tilde{X}_{t_{n+1}})) \middle| \tilde{X}_{t_n} = x \right], \quad (3.10)$$

where $\widehat{V}_j(t_{n+1}, \cdot)$ are approximations from previous time-steps, and $\widetilde{X}_{t_{n+1}}$ is an independent copy of the discretized process starting at state x and at time t_n . The M regression pairs become:

$$(X_{t_n}^i, Y_{t_n}^i), \quad Y_{t_n}^i = \frac{1}{m_Y} \sum_{\hat{i}=1}^{m_Y} \max_j (\Delta_t f_j(t_n, X_{t_n}^i) - c_{ij}(t_n, X_{t_n}^i) + \widehat{V}_j(t_{n+1}, \widetilde{X}_{t_{n+1}}^{i, \hat{i}})), \quad (3.11)$$

where m_Y trades computational cost against Monte Carlo variance — typically 1 in our simulations, but larger values are implied in our concentration bounds in Section 5.

3.5. Main algorithm and computational complexity. Computational scaling creates a fundamental trade-off between approximation quality and practical feasibility. The algorithm requires training $N \times D$ separate regression models — one for each time step and operating mode. With hundreds of time steps and multiple modes, this massive scaling means that a method’s computational efficiency must be taken into account along with theoretical approximation properties in determining overall performance. A simple method that trains quickly across hundreds of models can outperform a sophisticated method that provides better individual approximations but becomes computationally prohibitive when scaled.

The algorithm estimates $\widetilde{V}_i(t_0, x)$ by training regression models $\mathcal{R}_{n,i}$ that map state x to expected profit in mode j at time t_n . For notational convenience, define $\mathcal{R}_i(t_n, x) = \mathcal{R}_{n,i}(x)$ and denote the collection of all trained models by \mathcal{R} .

Algorithm 1 Value Function Approximation via Regression

- 1: Generate M simulated state trajectories $\{X_{t_0}^i, \dots, X_{t_N}^i\}_{i=1}^M$
 - 2: **for** $n = N, N-1, \dots, 1$ **do** ▷ Backward induction
 - 3: Extract states $\{X_{t_n}^1, \dots, X_{t_n}^M\}$ at time t_n
 - 4: For each $X_{t_n}^i$, simulate m_Y one-step transitions $\{\widetilde{X}_{t_{n+1}}^{i,k}\}_{k=1}^{m_Y}$
 - 5: **for** $j = 1, \dots, D$ **do** ▷ For each starting mode
 - 6: Compute targets: $Y_{j,t_n}^i = \frac{1}{m_Y} \sum_{k=1}^{m_Y} \max_l (\Delta t \cdot f_l(X_{t_n}^i, t_n) - c_{j,l}(X_{t_n}^i, t_n) + \mathcal{R}_l(t_{n+1}, \widetilde{X}_{t_{n+1}}^{i,k}))$
 - 7: Train regression model $\mathcal{R}_{n,j}$ using $\{(X_{t_n}^i, Y_{j,t_n}^i)\}_{i=1}^M$
 - 8: **end for**
 - 9: **end for**
-

The total computational cost is $O(N \times D \times (C_{\text{train}}(M, d) + M \times m_Y \times C_{\text{pred}}(d)))$, where C_{train} and C_{pred} are the training and prediction complexities for each model. Training complexity typically dominates, but the $M \times m_Y$ prediction calls during backward induction can create bottlenecks for expensive inference methods like k -nearest neighbors.

The specific complexities for each method appear in Table 1.

3.6. Metrics and comparisons. Since the true value function $V_i(x, t)$ is unknown, we evaluate our models using upper and lower bounds constructed from benchmark strategies.

Upper bound: A posteriori strategy. The *a posteriori* strategy μ^{ap} uses future knowledge to make optimal decisions — clearly inadmissible since it is not adapted to the process, but provides an upper bound on achievable performance. For a realized trajectory $\{X_0, X_1, \dots, X_N\}$, we define by backwards induction:

$$\mathcal{V}_i^{\text{ap}}(t_n) = \max_{j \in \{1, \dots, D\}} \left\{ f_j(t_n, X_n) \Delta t - c_{i,j}(t_n, X_n) + \mathcal{V}_j^{\text{ap}}(t_{n+1}) \right\},$$

where $\mathcal{V}_i^{\text{ap}}(t_N) = 0$ for all i . The corresponding strategy $\mu^{\text{ap}}(t_n)$ follows from (3.5), yielding the a posteriori value function:

$$V_i^{\text{ap}}(t_n, x) = J_i(t_n, x, \mu^{\text{ap}}(t_n)). \quad (3.12)$$

By Jensen’s inequality $V_i(t_n, x) \leq V_i^{\text{ap}}(t_n, x)$, no admissible strategy can beat complete knowledge of the future.

Lower bound: Myopic strategy. The greedy strategy ignores future consequences, maximizing only immediate payoffs. For $n < N$:

$$\mu^{\text{gr}}(t_n) \in \arg \max_{j \in \{1, \dots, D\}} \{f_j(t_n, X_n) \Delta t - c_{\mu^{\text{gr}}(t_{n-1}), j}(t_n, X_n)\}. \quad (3.13)$$

The greedy value function is:

$$V_i^{\text{gr}}(t_n, x) = J_i(t_n, x, \mu^{\text{gr}}(t_n)). \quad (3.14)$$

Since this strategy is adapted by construction, $V_i(t, x) \geq V_i^{\text{gr}}(t, x)$. We estimate both (3.12) and (3.14) by their empirical means.

Model benchmarking. Any reasonable regression model \mathcal{R} should satisfy:

$$V_i^{\text{gr}}(t_n, x) \leq \mathcal{R}_i(t_n, x) \leq V_i^{\text{ap}}(t_n, x). \quad (3.15)$$

Achieving the lower bound verifies non-trivial learning; approaching the upper bound indicates near-optimal performance given available information.

Strategy implementation. We implement strategies $\mu^{\mathcal{R}}$ derived from our regression models using (3.5). Let $S_j = \mathcal{R}_j(t_n, X_n) - c_{\mu^{\mathcal{R}}(t_n), j}(t_n, X_n)$. Then:

$$\mu^{\mathcal{R}}(t_n) = \begin{cases} \arg \max_{j \neq \mu^{\mathcal{R}}(t_{n-1})} S_j & \text{if } \max_{j \neq \mu^{\mathcal{R}}(t_{n-1})} S_j \geq S_{\mu^{\mathcal{R}}(t_{n-1})} \\ \mu^{\mathcal{R}}(t_{n-1}) & \text{otherwise} \end{cases} \quad (3.16)$$

Performance metrics. We evaluate models on three dimensions:

1. *Decision quality:* How often does our strategy match a posteriori-optimal switches?

$$Q_i^{\mathcal{R}} := \mathbb{E} \left[\frac{\sum_{\tau \in \mathcal{T}} \mathbb{1}_{\mu^{\mathcal{R}}(\tau) = \mu^{\text{ap}}(\tau)}}{N + 1} \mid \xi_0 = i \right]. \quad (3.17)$$

2. *Value capture:* What fraction of achievable value do we realize? We normalize the realized value:

$$\kappa_i^{\mathcal{R}}(t_n, x) := \frac{V_i^{\mathcal{R}}(t_n, x)}{V_i^{\text{ap}}(t_n, x)}, \quad (3.18)$$

where $V_i^{\mathcal{R}}(t_n, x) = J_i(t_n, x, \mu^{\mathcal{R}}(t_n))$ is the value achieved by following strategy $\mu^{\mathcal{R}}$.

3. *Internal consistency:* Does our value function accurately predict its own strategy's performance?

$$C_i^{\mathcal{R}}(t_n, x) := \frac{1}{1 + |V_i^{\mathcal{R}}(t_n, x) - \mathcal{R}_i(t_n, x)| / |V_i^{\text{ap}}(t_n, x)|}. \quad (3.19)$$

While decision quality and value capture measure actual performance, this measures another useful aspect: model calibration versus discrimination. A model can make good relative decisions (high decision quality) while having systematically biased value estimates. For instance, if a model overestimates all values by 50%, it may still rank decisions correctly and achieve good value capture, but managers cannot trust the absolute value predictions for budgeting, risk assessment, or comparing with alternative investments.

4. REGRESSION MODELS FOR OPTIMAL SWITCHING

The three challenges established in Section 3.4 — contaminated training targets, $N \times D$ computational scaling, and high-dimensional feature spaces — create distinct constraints on regression method selection. We evaluate eight regression approaches: linear models as natural baselines, local regression methods (k -NN), tree-based methods (Random Forests, LGBM), and neural networks. This selection tests different approaches to the computational, noise, and dimensional challenges inherent in optimal switching problems.

Computational scaling drives method selection. Training $N \times D$ models makes per-model training cost critical. Table 1 shows the scaling properties that determine practical feasibility. Methods like polynomial OLS with degree p suffer $O(Md^{2p})$ training costs that explode exponentially with both dimension and polynomial degree, making it completely infeasible beyond low-dimensional problems.

TABLE 1. Computational Complexity by Method

Method	Training	Prediction	Memory
OLS (degree p)	$O(Md^{2p})$	$O(d^p)$	$O(d^2)$
Ridge	$O(Md^2)$	$O(d)$	$O(d^2)$
LASSO	$O(Md^2)$	$O(d)$	$O(d^2)$
Random Forests	$O(M \log(M)T\sqrt{d})$	$O(T \log(M))$	$O(TM)$
LightGBM	$O(MdT)$	$O(T \log(M))$	$O(T + bd)$
k -NN	$O(Md)$	$O(Md + M \log(M))$	$O(Md)$
PCA- k -NN	$O(Md^2) + O(Md)$	$O(M)$	$O(Md)$
Neural Networks	$O(Mdhe)$	$O(dh)$	$O(dh + h^2)$

Note: M : samples, d : dimension, T : trees, h : hidden width, e : epochs, p : polynomial degree, b : bins in histogram

Fig. 1 shows training and prediction times for models using the hyperparameters from our experiments Section 3.4.

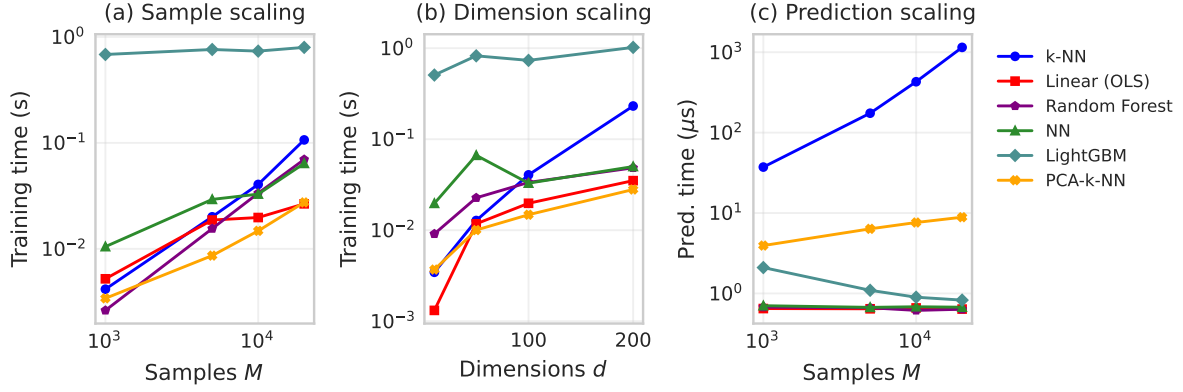


FIGURE 1. Model scaling analysis: (a) training time vs samples, (b) training time vs dimensions, (c) prediction time. Training times reflect the cost of training one model for a single time step and mode; total algorithm runtime follows the complexity formula in Section 3.5. Our algorithm in Section 3.5 required minutes to an hour depending on the specific regression model, hyperparameters, and which experiment we ran.

Noisy training data favors robust methods. Estimates of (3.9) contain simulation error that compounds across dynamic programming recursion. Methods that overfit to this noise, such as high degree polynomials or deep networks, can produce unstable decision boundaries.

High dimensions break distance-based methods Standard k -NN fails in dimensions ~ 10 due to distance concentration — all points become equidistant. We test PCA- k -NN as a dimensionality reduction approach, trading information loss for meaningful nearest neighbor distances.

4.1. Linear models. All linear models are configured to first standardize the input features to zero mean and unit variance. This improves numerical stability and ensures regularization is applied uniformly across features.

Ordinary Least Squares serves as our baseline, using polynomial degree 6 for $d \leq 2$ to capture nonlinear decision boundaries, and degree 1 otherwise to avoid parameter explosion. All linear models include input standardization for numerical stability.

Ridge regression ($\lambda = 0.1$) handles correlated state variables common in optimal switching problems, where for instance asset prices move together. The L2 penalty stabilizes estimates in these ill-conditioned settings without eliminating potentially useful features.

LASSO regression ($\lambda = 0.1$) performs automatic feature selection through L1 penalties, identifying situations where switching decisions depend on few key variables rather than the full state space. This sparsity can improve both interpretability and performance in higher dimensions.

4.2. Tree-based methods.

Random forests (25 trees, depth 3) reduce noise through bootstrap aggregation-averaging predictions across trees trained on different data subsets smooths Monte Carlo error. Shallow trees prevent individual trees from overfitting while ensemble averaging provides stability across the hundreds of models required for optimal switching.

LightGBM (200 iterations, learning rate 0.05) achieves robustness through regularization: L2 penalties, 80% data sub-sampling, minimum 100 points per leaf. The histogram approach also cuts memory usage in high dimensions.

4.3. Local regression Methods.

k -Nearest Neighbors ($k = 10$) averages over neighborhoods, naturally smoothing Monte Carlo noise without distributional assumptions. Works well until dimensionality breaks distance metrics.

PCA- k -NN (6 components) projects to principal components before computing distances-trading information for meaningful proximity measures in high dimensions.

4.4. Neural networks.

Architecture exploration. We explored various neural network configurations to ensure fair comparison, testing ReLU and Tanh activations, depths up to 4 layers, widths up to 512 units, different optimizer parameters (learning rates, decay schedules), with and without dropout, variable-breadth architectures, and both with and without early stopping.

Based on this exploration, we selected architectures up to 128 hidden units and 2 layers, using dropout for regularization and ADAM optimization with exponential learning rate decay. These configurations provided the best performance across experiments while maintaining training times comparable to other methods.

Neural networks exploit temporal structure through backward initialization: parameters for time-step n initialize from time-step $n + 1$ with small Gaussian perturbations ($\theta_n = \theta_{n+1} + 0.005 \cdot \mathcal{N}(0, 1)$). This leverages the assumption that $\mathcal{R}_{n,i} \approx \mathcal{R}_{n+1,i}$ since value functions change smoothly over small time-intervals Δt .

More detailed specifications of architectures, implementation details, and a summary of hyperparameters for the different regression models can be found in Appendix B.

5. THEORETICAL GUARANTEES FOR THE LONGSTAFF-SCHWARTZ ALGORITHM

In this section we provide theoretical guarantees for the Longstaff-Schwartz algorithm when the regression method is k -nearest neighbor regression (foreshadowing the results of our numerical experiments, this regression model does perform well in practice as well). We first treat the case when the transition kernel is sub-Gaussian and later cover the sub-exponential case which covers 1-d jump-diffusion.

The k -nearest neighbor estimator at time-step n and mode j is defined by:

$$R_{n,j}(x) = \sum_{i \in \mathcal{N}(x)} Y_{t_n}^i, \quad (5.1)$$

where $\mathcal{N}(x)$ are the indices of the k nearest neighbors of x in the training set.

5.1. The sub-Gaussian case. We will here assume that our Markov process has a transition density that satisfies the following bounds: For a fixed Δt , there exists constants $\lambda_1, \lambda_2 > 0$ such

that for every $x, y \in \mathbb{R}^d$ we have

$$\begin{aligned} |\rho(x, t; y, t + \Delta_t)| &\leq \frac{1}{\lambda_1} \exp(-\lambda_1 \|x - y\|^2), \\ |\nabla_x \rho(x, t; y, t + \Delta_t)| &\leq \frac{1}{\lambda_2} \exp(-\lambda_2 \|x - y\|^2). \end{aligned} \quad (5.2)$$

Remark 5.1. If X_t is a diffusion process, the above estimates hold under rather mild conditions on the drift and diffusion terms.

Recall that $D_T = \{X_{t_0}^i, \dots, X_{t_N}^i; i = 1, \dots, M\}$ is the set of all states at all times for the M independent trajectories. Then if $\widehat{V}_i(t_{n+1}, x)$ is an approximation of the continuation value $V_i(t_{n+1}, x)$ then the target value function is

$$\widetilde{V}_i(t_n, x) = \mathbb{E} \left[\max_j (\Delta_t f_j(t_n, x) - c_{ij}(t_n, x) + \widehat{V}_j(t_{n+1}, \widetilde{X}_{t_{n+1}})) \mid \widetilde{X}_{t_n} = x \right]. \quad (5.3)$$

In the above $\widetilde{X}_{t_{n+1}}$ is an independent copy of the process X_t at time t_{n+1} . Let k be a positive integer then, the k -NN estimator, see (5.1) for functional form, of $\widetilde{V}_i(t_n, x)$ using the data pairs in (3.11) is given by

$$\widehat{\widetilde{V}}_i(t_n, x) = \frac{1}{km_Y} \sum_{s \in \mathcal{N}_{t_n}(x)} \sum_{\hat{s}=1}^{m_Y} \max_j (\Delta_t f_j(t_n, X_{t_n}^s) - c_{ij}(t_n, X_{t_n}^s) + \widehat{V}_j(t_{n+1}, \widetilde{X}_{t_{n+1}}^{s, \hat{s}})), \quad (5.4)$$

where $(\widetilde{X}_{t_{n+1}}^{s, 1}, \dots, \widetilde{X}_{t_{n+1}}^{s, m_Y})$ are independent copies of the process X_t started at $X_{t_n}^s$ at time t_n and $\mathcal{N}_{t_n}(x)$ is the set of k -nearest neighbors of x out of the set D_T at time t_n with respect to the Euclidean distance.

The final estimate at time t_n of the approximate value function $\widetilde{V}_i(t_n, x)$ is the following truncated version of $\widehat{\widetilde{V}}_i(t_n, x)$,

$$\widehat{V}_i(t_n, x) = \min\{\widehat{\widetilde{V}}_i(t_n, x), 2C_0(\|x\| + 1)\}, \quad (5.5)$$

where C_0 is a given constant.

Remark 5.2. The way truncated value function $\widehat{V}_i(t_n, x)$ is defined is to ensure that the growth condition in the following theorem is always satisfied. Although the constant C_0 needs to grow as n becomes smaller. Thus, the following theorem gives us the one-step error in supremum norm inside a fixed cube Q .

Theorem 5.3. Let (5.2) hold, assume that $0 \leq \widehat{V}_i(t_{n+1}, x) \leq L(\|x\| + 1)$ for some $L > 0$ and assume that the functions $f_j \geq 0$ and c_{ij} ($c_{ii} = 0$) are globally Lipschitz continuous in x (with constant L) and satisfies the same growth condition as $\widehat{V}_i(t_{n+1}, x)$. Then for any fixed bounded set $Q \subset \mathbb{R}^d$ there exists positive constants C_0 (used in (5.5)), C_1 , C_2 and σ , depending only on d , L , Q , λ_1 and λ_2 , such that for any $\delta > 0$ it holds

$$\begin{aligned} \mathbb{P}(\sup_{x \in Q} |\widehat{V}_i(t_n, x) - \widetilde{V}_i(t_n, x)| \geq \delta) &\leq 2 \binom{M}{k} \exp\left(-\frac{km_Y \delta^2}{6\sigma^2}\right) \\ &\quad + \begin{cases} C_1 \frac{|Q|}{\delta^d} \exp\left(-\frac{M\left(\frac{M-k}{M} - \sup_Q p_{\delta/(4C_2)}^c\right)_+^2}{2}\right) & \text{if } \delta/C_2 \leq 1, \\ C_1 \frac{|Q|}{\delta^{d/2}} \exp\left(-\frac{M\left(\frac{M-k}{M} - \sup_Q p_{\sqrt{\delta/(4C_2)}}^c\right)_+^2}{2}\right) & \text{if } \delta/C_2 > 1, \end{cases} \end{aligned}$$

where $p_r^c = \mathbb{P}(X_{t_n} \notin B(x, r))$, where $B(x, r)$ is the Euclidean ball of radius r centered at $x \in \mathbb{R}^d$ and $|Q|$ is the volume of the set Q .

In the above theorem we have two quantities that restrict the values of k and m_Y in order for the estimate to become useful. The first is that we need

$$\frac{M-k}{M} - p_0 > 0 \implies k < M(1 - p_0),$$

where $p_0 = \sup_Q p_{\delta/(4C_2)}^c$ in the small δ case and $p_0 = \sup_Q p_{\sqrt{\delta/(4C_2)}}^c$ in the large δ case. As such k cannot be too large. The reason for this is that if we have too many neighbors the k -nearest neighbor regression smooths out the function too much and will not be close to the target value function.

On the other hand, the noise induced by the one-step simulations is controlled by m_Y . The averaging effect of k -nearest neighbor regression will provide some weak concentration for large k but unless m_Y is large enough the estimates are not strong enough to provide a good approximation. Specifically, we need that

$$\binom{M}{k} \exp\left(-\frac{km_Y\delta^2}{6\sigma^2}\right) \rightarrow 0.$$

Assuming that the first condition gives $k < M/2$ we can use the following bound for the binomial coefficient $\binom{M}{k} \leq (eM/k)^k$ to get that we need

$$\left((\log(M/k) + 1) - \frac{m_Y\delta^2}{6\sigma^2}\right) < 0.$$

Theorem 5.4. *Under the same assumptions of Theorem 5.3 we have that for any fixed point $x \in \mathbb{R}^d$, that there exists positive constants C_0 (used in (5.5)), C_1 , C_2 and σ , depending only on d , L , Δ_t , $|x|$, λ_1 and λ_2 , such that for any $\delta > 0$ it holds*

$$\begin{aligned} \mathbb{P}(|\widehat{V}_i(t_n, x) - \widetilde{V}_i(t_n, x)| \geq \delta) &\leq 2 \exp\left(-\frac{km_Y\delta^2}{6\sigma^2}\right) \\ &\quad + 2 \begin{cases} \exp\left(-\frac{M\left(\frac{M-k}{M} - p_{\delta/(4C_2)}^c\right)_+^2}{2}\right) & \text{if } \delta/C_2 \leq 1, \\ \exp\left(-\frac{M\left(\frac{M-k}{M} - p_{\sqrt{\delta/(4C_2)}}^c\right)_+^2}{2}\right) & \text{if } \delta/C_2 > 1, \end{cases} \end{aligned}$$

where $p_r^c = \mathbb{P}(X_{t_n} \notin B(x, r))$.

We note that the above theorem has a better concentration property compared to Theorem 5.3, specifically we can take $m_Y = 1$ as long as $k \rightarrow \infty$ as $M \rightarrow \infty$ and the classical assumption that $M/k \rightarrow 0$ as $M \rightarrow \infty$ is satisfied. In this case, then for large enough M we have

$$\mathbb{P}(|\widehat{V}_i(t_n, x) - \widetilde{V}_i(t_n, x)| \geq \delta) \leq 4 \exp\left(-\frac{k\delta^2}{6\sigma^2}\right).$$

5.2. The sub-exponential case. We will here assume that our Markov process has a transition density that satisfies the following bounds: For a fixed Δt , there exists constants $\lambda_1, \lambda_2 > 0$ such that for every $x, y \in \mathbb{R}^d$ we have

$$\begin{aligned} |\rho(x, t; y, t + \Delta t)| &\leq \frac{1}{\lambda_1} \exp(-\lambda_1 \|x - y\|), \\ |\nabla_x \rho(x, t; y, t + \Delta t)| &\leq \frac{1}{\lambda_2} \exp(-\lambda_2 \|x - y\|). \end{aligned} \tag{5.6}$$

Remark 5.5. In Appendix E we show that the above estimates hold for jump-diffusion processes that only have jumps in one direction.

Theorem 5.6. Let (5.6) hold, assume that $0 \leq \widehat{V}_i(t_{n+1}, x) \leq L(\|x\| + 1)$ for some $L > 0$ and assume that the functions $f_j \geq 0$ and c_{ij} ($c_{ii} = 0$) are globally Lipschitz continuous in x and satisfies the same growth condition as $\widehat{V}_i(t_{n+1}, x)$. Then for any fixed bounded set $Q \subset \mathbb{R}^d$ there exists positive constants C_0 (used in (5.5)), C_1 , C_2 and σ , such that for any $\delta > 0$ it holds

$$\begin{aligned} \mathbb{P}(\sup_{x \in Q} |\widehat{V}_i(t_n, x) - \widetilde{V}_i(t_n, x)| \geq \delta) &\leq 2 \binom{M}{k} \max \left\{ \exp \left(-\frac{km_Y \delta^2}{6\sigma^2} \right), \exp \left(-\frac{km_Y \delta}{4\sigma} \right) \right\} \\ &\quad + \begin{cases} C_1 \frac{|Q|}{\delta^d} \exp \left(-\frac{M \left(\frac{M-k}{M} - \sup_Q p_{\delta/(4C_2)}^c \right)_+^2}{2} \right) & \text{if } \delta/C_2 \leq 1, \\ C_1 \frac{|Q|}{\delta^{d/2}} \exp \left(-\frac{M \left(\frac{M-k}{M} - \sup_Q p_{\sqrt{\delta/(4C_2)}}^c \right)_+^2}{2} \right) & \text{if } \delta/C_2 > 1, \end{cases} \end{aligned}$$

where $p_r^c = \mathbb{P}(X_{t_n} \notin B^c(x, r))$.

Remark 5.7. We note that one can extend Theorem 5.4, using the moment method (see for instance [BLM13]), to the case of when (5.6) is replaced by an upper bound of the form $1/K(\|x - y\|)$ where K is a non-negative polynomial. In this case the decay of first term on the right-hand side in Theorem 5.4 will depend on the growth of K .

6. NUMERICAL EXPERIMENTS

We test machine learning methods in the Longstaff-Schwartz algorithm across four experiments to evaluate different aspects of method performance: robustness across problem types, multiscale planning and dimensionality scaling.

Our experimental design uses established examples from [CL08, ACLP14, BCN23], and a new artificial problem that requires multi-timescale planning. All experiments use a 90/10 train/validation split and models, except neural networks, had minimal hyperparameter tuning to assess out-of-the-box performance.

Overview of examples used:

- **Carmona-Ludkovski (CL) and ACLP:** Established examples from the optimal switching literature
- **Artificial planning (BSP):** Designed to test scenarios where myopic strategies should fail due to multi-timescale interactions
- **High-dimensional CL (HCL):** Tests dimensional scaling by extending CL to higher dimensions

6.1. Experiment 1: Carmona-Ludkovski (CL). The Carmona-Ludkovski experiment models gas-fired power plant management, following the formulation in [CL08] as adjusted by [BCN23].

The model captures interplay between electricity price P_t and gas price G_t , incorporating market features such as mean reverting dynamics, price correlation and electricity price spikes. The state process $X_t = (P_t, G_t)$ combines a jump-diffusion process for electricity price P_t and a diffusion process for gas price G_t . In differential form, the dynamics are given by

$$dX_t = \mu(X_t)dt + \sigma(X_t)dW_t + dJ_t, \quad (6.1)$$

where $W_t \in \mathbb{R}^2$ is a standard two-dimensional Brownian motion. The jump process J_t affects only the first dimension (electricity price) and is defined as:

$$J_t = \sum_{i=1}^{N_t} (e^{Y_i} - 1)e_1, \quad N_t \sim \text{Poisson}(32t), \quad Y_i \sim \text{Exponential}(10), \quad (6.2)$$

where e_1 denotes the first standard basis vector in \mathbb{R}^2 . The drift function $\mu(X_t)$ captures the mean-reverting behavior of the electricity and gas prices:

$$\mu(X_t) = \begin{pmatrix} 5P_t(\log 50 - \log P_t) \\ 2G_t(\log 6 - \log G_t) \end{pmatrix} \quad (6.3)$$

The diffusion function incorporates price dependent volatility and correlation:

$$\sigma(X_t) = \begin{pmatrix} 0.5P_t & 0 \\ 0.32G_t & 0.24G_t \end{pmatrix}. \quad (6.4)$$

Managing the power plant, we have three production modes: off, half capacity, and full capacity. The payoff functions for the three modes are:

$$f_j(t, X_t) = \begin{cases} -1, & \text{if } j = 1 \\ 0.438(P_t - 7.5G_t) - 1.1, & \text{if } j = 2 \\ 0.876(P_t - 10G_t) - 1.2, & \text{if } j = 3. \end{cases} \quad (6.5)$$

The switching-cost from mode i to mode j (ramping up or down production) is:

$$c_{ij}(t, X_t) = \begin{cases} 0, & \text{if } i = j \\ 0.01G_t + 0.001, & \text{if } i \neq j. \end{cases} \quad (6.6)$$

The model parameters used in our simulations are summarized in Table 2. The initial value X_0

TABLE 2. Model parameters for the CL example

Parameter	Value	Description
d	2	Dimension of random process
D	3	Number of modes
M	50000	Number of trajectories
N	180	Number of time points
m_Y	1	Number of one-step trajectories in training
t_{start}	0	Start time
t_{end}	0.25	End time
Δt	$(t_{\text{end}} - t_{\text{start}})/N$	Time step
λ_{Poisson}	32	Average number of jumps in electricity prices per year
λ_{exp}	10	Inverse of average intensity of jumps

is set as:

$$X_0 = (50, 6) + \epsilon, \quad \epsilon \sim \mathcal{N}(0, 0.01^2 I) \quad (6.7)$$

Remark 6.1. Our implementation uses a jump intensity of $\lambda = 32$ in the electricity price process, compared to $\lambda = 8$ in the original models of [CL08] and [BCN23]. This modification was motivated by preliminary numerical experiments, which revealed that lower jump intensities resulted in mostly static switching strategies, with most trajectories staying in the same mode through the time horizon. The higher jump frequency induces more frequent transitions between operational modes, allowing for a more thorough examination of the switching boundaries and how the different models perform in these regions.

6.2. Experiment 2: Aïd-Campi-Langrené-Pham (ACLP). The ACLP experiment tests method performance on a higher-dimensional fuel management problem [ACLP14], as adapted in [BCN23], where power plants optimize across multiple fuel types with varying availability and costs. Unlike the two-dimensional CL problem, this 9-dimensional setting challenges methods to more handle complex state interactions while maintaining decision quality.

The model captures a power plant manager choosing between four operational modes, each representing different fuel allocation strategies. The state process $X_t = (Z_t, S_t) \in \mathbb{R}^9$ tracks demand/availability factors (Z_t) and various fuel and electricity prices (S_t).

In more detail: The state process $X_t = (Z_t, S_t) \in \mathbb{R}^9$ combines two components:

- $Z_t = (Z_t^0, Z_t^1, Z_t^2, Z_t^3)$ represents demand and availability rates of three fuel types.
- $S_t = (S_t^0, S_t^1, S_t^2, S_t^3, S_t^4)$ represents various prices.

These components determine

- Electricity demand $D_t = Z_t^0 + H^0(t)$,
- Availability rates $A_t^\phi = \kappa(Z_t^\phi + H_t^\phi)$ for $\phi = 1, 2, 3$,
- Fuel costs and electricity prices S_t ,

where $H^0(t)$ and $H^\phi(t)$ are seasonal adjustments that ensure demand and availability rates stay within certain bounds, and κ is the standard normal cumulative distribution function, setting availability rates between 0 and 1.

The dynamics follow a jump-diffusion process:

$$\begin{aligned} dZ_t &= -\alpha \odot Z_t dt + \beta dW_t^1, \quad \beta \in \mathbb{R}^{4 \times 4} \\ dS_t &= \Xi S_t dt + s_\sigma \text{diag}(S_t) dW_t^2 + S_t \odot dJ_t, \quad \Xi \in \mathbb{R}^{5 \times 5} \end{aligned} \quad (6.8)$$

where \odot denotes the Hadamard product (element-wise multiplication), $\alpha \in \mathbb{R}^4$ is a mean-reversion vector, β represents volatility, and Ξ captures price correlations and $W_t = (W_t^1, W_t^2)$ is a 9-dimensional Brownian motion. The jump process affects only the price components and follows:

$$J_t^i = \sum_{k=1}^{N_t^i} (e^{Y_k^i} - 1), \quad N_t^i \sim \text{Poisson}(\lambda_i t), \quad Y_k^i \sim \text{Exponential}(\lambda_i), \quad i = 1, \dots, n_{\text{prices}}. \quad (6.9)$$

Now we define the payoff functions and switching costs. The plant manager operates in four distinct modes, each representing a specific allocation of capacity across different fuel sources. These modes are encoded as rows in a capacity matrix $C \in \mathbb{R}^{4 \times 3}$, where $C_{j,k}$ represents the capacity allocated to fuel type k in mode j . The payoff function $f_j : \mathbb{R}^9 \times [0, 1] \rightarrow \mathbb{R}$ for mode j is given by:

$$f_j(t, X_t) = \min \left\{ \sum_{k=1}^3 C_{j,k} A_t^k, D_t \right\} S_t^4 - \sum_{k=1}^3 C_{j,k} (h_{\text{CO2},k} S_t^0 + h_{\text{tech},k} S_t^k) \quad (6.10)$$

where $C_{j,k} A_t^k$ represents the effective capacity for fuel type k in mode j , adjusted by its availability factor. The first term calculates revenue as the minimum of total effective capacity and demand, multiplied by the electricity price. The second term represents operational costs, including both carbon dioxide emissions and technology-specific costs.

The cost of switching from mode i to mode j is defined by:

$$c_{ij}(t, X_t) = \frac{1}{3} \sum_{k=1}^3 S_t^k \cdot \mathbb{1}_{C_{i,k} \neq C_{j,k}} + 0.001 \quad (6.11)$$

where $\mathbb{1}_{C_{i,k} \neq C_{j,k}}$ is the indicator function that equals 1 when the capacity allocation for fuel k differs between modes i and j , and 0 otherwise. This cost reflects the expenses of fuel replacement during mode transitions, proportional to current fuel prices, plus a small fixed cost.

The starting distribution is

$$(70, 1, 1, 0, 20, 60, 40, 20, 120) + \epsilon, \quad \epsilon \sim \mathcal{N}(0, 0.005^2 I) \quad (6.12)$$

The exact values of the capacity matrix C , and other parameters $h_{\text{CO2},k}$, $h_{\text{tech},k}$, β , s_{long} , s_α , and s_σ can be found in the code [And25], and the main experiment parameters are found in Table 3

TABLE 3. Model parameters for the ACLP example

Parameter	Value	Description
d	9	Dimension of random process
N	90	Number of time steps
J	4	Number of modes
M	50000	Number of trajectories
m_Y	1	Number of one-step trajectories in training
t_{start}	0	Start time
t_{end}	1	End time
Δt	$(t_{\text{end}} - t_{\text{start}})/N$	Time step
λ_{Poisson}	12	Average number of jumps in electricity prices per year
λ_{exp}	15	Inverse of average intensity of jumps

6.3. Experiment 3: Banded Shift Process (BSP). The BSP experiment tests whether methods can learn forward-planning strategies that outperform more greedy approaches. We design a one-dimensional process where optimal modes form spatial bands that shift over time, requiring incremental transitions rather than immediate jumps to maximize long-term value.

The state process $X_t \in \mathbb{R}$ follows mean-reverting dynamics with time-varying mean:

$$dX_t = -\alpha(X_t - \mu(t))dt + \sigma(X_t)dW_t \quad (6.13)$$

where W_t is a standard Brownian motion. The model components are defined as follows:

$$\mu(t) = \sin(2\pi t) \quad (\text{time-varying mean}) \quad (6.14)$$

$$\alpha = 0.5 \quad (\text{mean reversion speed}) \quad (6.15)$$

$$\sigma(X_t) = 0.5 + 0.2|X_t| \quad (\text{state-dependent volatility}) \quad (6.16)$$

The controller chooses between 10 operational modes in a setting designed to punish myopic decisions. We divide the state space into adjacent bands, where each mode achieves maximum payoff (1.0) in its designated band and reduced payoff (0.2) in neighboring bands.

Specifically, the state range $[-2, 2]$ is partitioned into bands of width 0.4, with mode j optimal when X_t falls in band j . Adjacent modes receive moderate payoffs, creating a local neighborhood structure. The payoff function $f_j : \mathbb{R} \times [0, 1] \rightarrow \mathbb{R}$ is:

$$f_j(t, X_t) = \begin{cases} 1.0, & \text{if } j = \lfloor \frac{X_t+2}{0.4} \rfloor + 1 \text{ and } -2 \leq X_t \leq 2 \\ 0.2, & \text{if } j = \lfloor \frac{X_t+2}{0.4} \rfloor \text{ or } j = \lfloor \frac{X_t+2}{0.4} \rfloor + 2 \\ 0, & \text{otherwise} \end{cases} \quad (6.17)$$

Switching costs increase with mode distance but plateau, creating incentives for gradual transitions:

$$c_{ij}(t, X_t) = \begin{cases} 0, & \text{if } i = j \\ 0.05 \min(|i - j|, 3), & \text{if } i \neq j \end{cases} \quad (6.18)$$

The combination of banded payoffs and distance-dependent switching costs creates a challenging control problem, that should be difficult for greedy algorithms. For instance, as X_t changes, a greedy controller would immediately shift to the new highest payoff (minus switching cost) mode, whereas an optimal controller might make incremental transitions, temporarily accepting lower rewards to maximize cumulative profits. Furthermore, the time-varying mean and state-dependent volatility introduce additional complexities, requiring the controller to adapt and anticipate changing dynamics. The initial distribution of X_0 is set as:

$$X_0 = 0 + \epsilon, \quad \epsilon \sim \mathcal{N}(0, 0.5^2) \quad (6.19)$$

The experiment parameters summarized in Table 4

TABLE 4. Model parameters for the BSP experiment

Parameter	Value	Description
d	1	Dimension of random process
J	10	Number of modes
K	20000	Number of trajectories
N	36	Number of time points
m_Y	1	Number of one-step trajectories in training
t_{start}	0	Start time
t_{end}	1	End time
Δt	$(t_{\text{end}} - t_{\text{start}})/N$	Time step

6.4. Experiment 4: High dimensional extension of Carmona-Ludkovski (HCL). The HCL experiment tests method performance as state dimensions increase from 2 to 50, extending the CL power plant model [BCN23] to higher-dimensional settings. This experiment isolates dimensional scaling effects by maintaining the same three-mode structure while adding correlated state variables.

The high-dimensional state process $X_t \in \mathbb{R}^d$ preserves the jump-diffusion structure of the original CL model, with electricity price jumps affecting only the first dimension and mean-reverting dynamics for all components:

$$dX_t = \mu(X_t)dt + \sigma(X_t)dW_t + dJ_t, \quad (6.20)$$

where $W_t \in \mathbb{R}^d$ is a standard d -dimensional Brownian motion, and J_t is a jump process only affecting the first dimension (price of electricity). The drift and diffusion functions are given by

$$\mu(X_t) = \kappa \odot X_t \odot (\log(X_0) - \log(X_t)), \quad (6.21)$$

$$\sigma(X_t) = \Sigma \quad (6.22)$$

where \log is applied element-wise, $\kappa = (5, 2, 2, \dots, 2) \in \mathbb{R}^d$, and Σ is the constant matrix

$$\Sigma = \begin{bmatrix} 0.5 & 0 & 0 & \cdots & 0 \\ 0.32 & 0.24 & 0 & \cdots & 0 \\ 0.32 & 0 & 0.24 & \cdots & 0 \\ \vdots & \vdots & \vdots & \ddots & \vdots \\ 0.32 & 0 & 0 & \cdots & 0.24 \end{bmatrix}. \quad (6.23)$$

There is thus state dependent volatility, and correlation between prices in this model. The jump process J_t is defined as:

$$J_t = \sum_{i=1}^{N_t} (e^{Y_i} - 1)e_1, \quad N_t \sim \text{Poisson}(\lambda_{\text{Poisson}}t), \quad Y_i \sim \text{Exponential}(1/\lambda_{\text{exp}}) \quad (6.24)$$

where e_1 is the unit vector in the first dimension.

The power plant operation maintains the three modes in the original CL problem, each representing differing capacities of the power plant. The plant is off (mode 1), at half capacity (mode 2) or at full capacity (mode 3). The payoff function $f_j : \mathbb{R}^d \times [0, 1]$, $j = 1, 2, 3$, for mode j is:

$$f_j(t, X_t) = a_j X_{1,t} + b_j \bar{X}_{2:d,t} + c_j \quad (6.25)$$

where $\bar{X}_{2:d,t} = \frac{1}{d-1} \sum_{i=2}^d X_{i,t}$, is the mean of all dimensions except the first one. The constants a_j , b_j , and c_j are defined as:

$$\begin{bmatrix} a_1 & a_2 & a_3 \\ b_1 & b_2 & b_3 \\ c_1 & c_2 & c_3 \end{bmatrix} = \begin{bmatrix} 0 & 0.438 & 0.876 \\ 0 & -3.285 & -8.76 \\ -1 & -1.1 & -1.2 \end{bmatrix}. \quad (6.26)$$

The cost of switching from mode i to mode j is:

$$c_{ij}(t, X_t) = \begin{cases} 0, & \text{if } i = j \\ 0.011, & \text{if } i \neq j \end{cases} \quad (6.27)$$

The initial value X_0 is defined as:

$$X_0 = (50, 6, 6, \dots, 6) \quad (6.28)$$

The experiment parameters can be seen in Table 5

TABLE 5. Model parameters for the HCL experiment

Parameter	Value	Description
d	variable	Dimension of random process
D	3	Number of modes
M	20000	Number of trajectories
N	180	Number of time points
m_Y	1	Number of one-step trajectories in training
t_{start}	0	Start time
t_{end}	0.25	End time
Δt	$(t_{\text{end}} - t_{\text{start}})/N$	Time step
λ_{Poisson}	32	Poisson process intensity
λ_{exp}	10	Inverse intensity of exponential jumps

7. RESULTS OF NUMERICAL EXPERIMENTS

7.1. Model performance results. We evaluate performance mainly using the three metrics: Decision quality $Q^{\mathcal{R}}$, value capture $\kappa^{\mathcal{R}}$, and internal consistency $C^{\mathcal{R}}$ (detailed in Section 3.6).

k -NN achieves robust near-optimal decisions across all problem types. Despite its simplicity, k -NN consistently ranks among top performers for decision quality and value capture across all experiments. In higher dimensions, PCA- k -NN maintains this performance while more complex methods deteriorate significantly (Figs. 2 and 2b). This robustness extends across very different problem structures-from simple to complex switching regimes.

High-quality decisions without accurate value function approximation. The high-dimensional Carmona-Ludkovski (HCL) experiment reveals a disconnect between prediction accuracy and decision quality. While k -NN achieves high quality decisions and almost full value capture (Fig. 2b), its internal consistency lags significantly behind linear models and random forests (Fig. 2b).

k -NN and LGBM accurately capture optimal decision regions In the CL experiment where we can visualize decision boundaries (Fig. 5), the top performers k -NN and LGBM successfully identify regions for optimal switching decisions. In contrast, neural networks exhibit temporal instability, their boundaries shift significantly across time-steps, sometimes aligning with optimal regions, sometimes not.

Training difficulty concentrates in the middle time horizon. Loss curves (Fig. 6) consistently show that regression becomes most challenging in intermediate time steps, with easier fitting at both initial conditions and terminal states.

8. DISCUSSION AND CONCLUSION

8.1. Interpretation of numerical results. The regression models that performed well identified near-optimal decision boundaries and mode-switching behavior. However, for k -NN in higher dimension this boundary detection success came with a systematic prediction bias problem. One explanation is that k -NN’s local averaging creates constant extrapolation at domain boundaries, failing to capture trends as states approach underexplored regions of state-space.

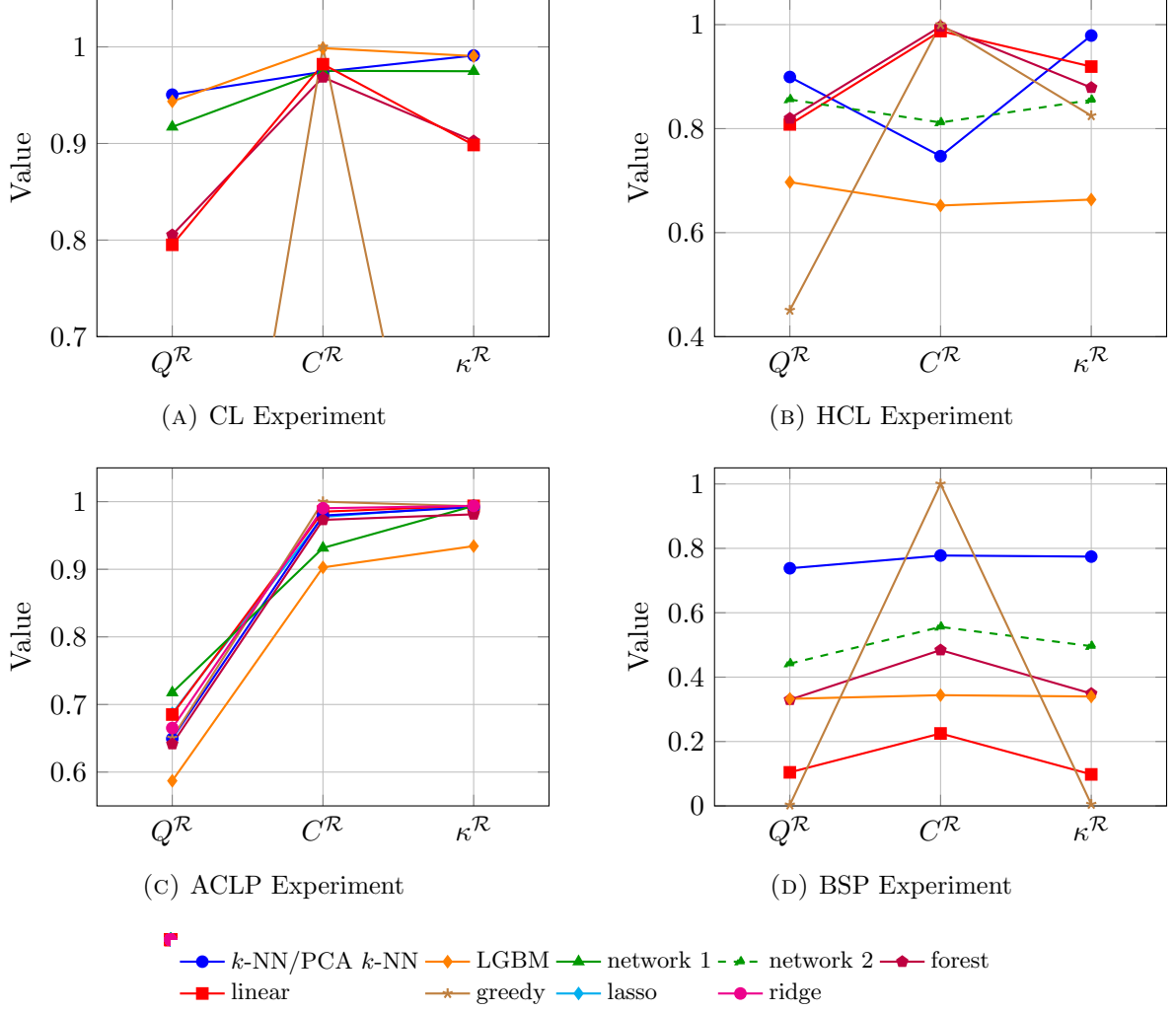


FIGURE 2. Performance metrics across different strategies for four experiments when starting in state 1: (a) CL experiment (Section 6.1), (b) High-dimensional CL experiment (Section 6.4), (c) ACLP experiment (Section 6.2), and (d) BSP experiment (Section 6.3). Starting values for paths were generated according to the same distributions as in the respective equations of X_0 for each experiment. For Internal Consistency and Value Capture, we have taken the mean at time t_0 over all paths. Total paths generated for each experiment was 1000. Among the linear models, we have only plotted the best performing one.

Decision boundary stability varied between methods. Despite our exploration of neural network architectures (different depths, widths, activations, and regularization schemes), networks consistently exhibited instability both with regard to hyperparameter changes and across time steps, with decision boundaries jumping discontinuously between steps (Fig. 5). All other models demonstrated stable training behavior, producing similar results under small hyperparameter variations -an important advantage when training hundreds of models in the backward induction process.

The loss curves (Fig. 6) indicate why no single method dominates: regression difficulty changes systematically over time. Because terminal conditions are simple (just equal to 0), the first regression problem are easy to solve. At early time-steps in our random processes, the state domain is concentrated, which also make regression easier. This domain then generally expands due to diffusion, specifically the term p_r^c (in Theorems 5.3, 5.4 and 5.6) increases with time for a fixed r . Moreover, in the Longstaff-Schwartz backward induction, each regression inherits the

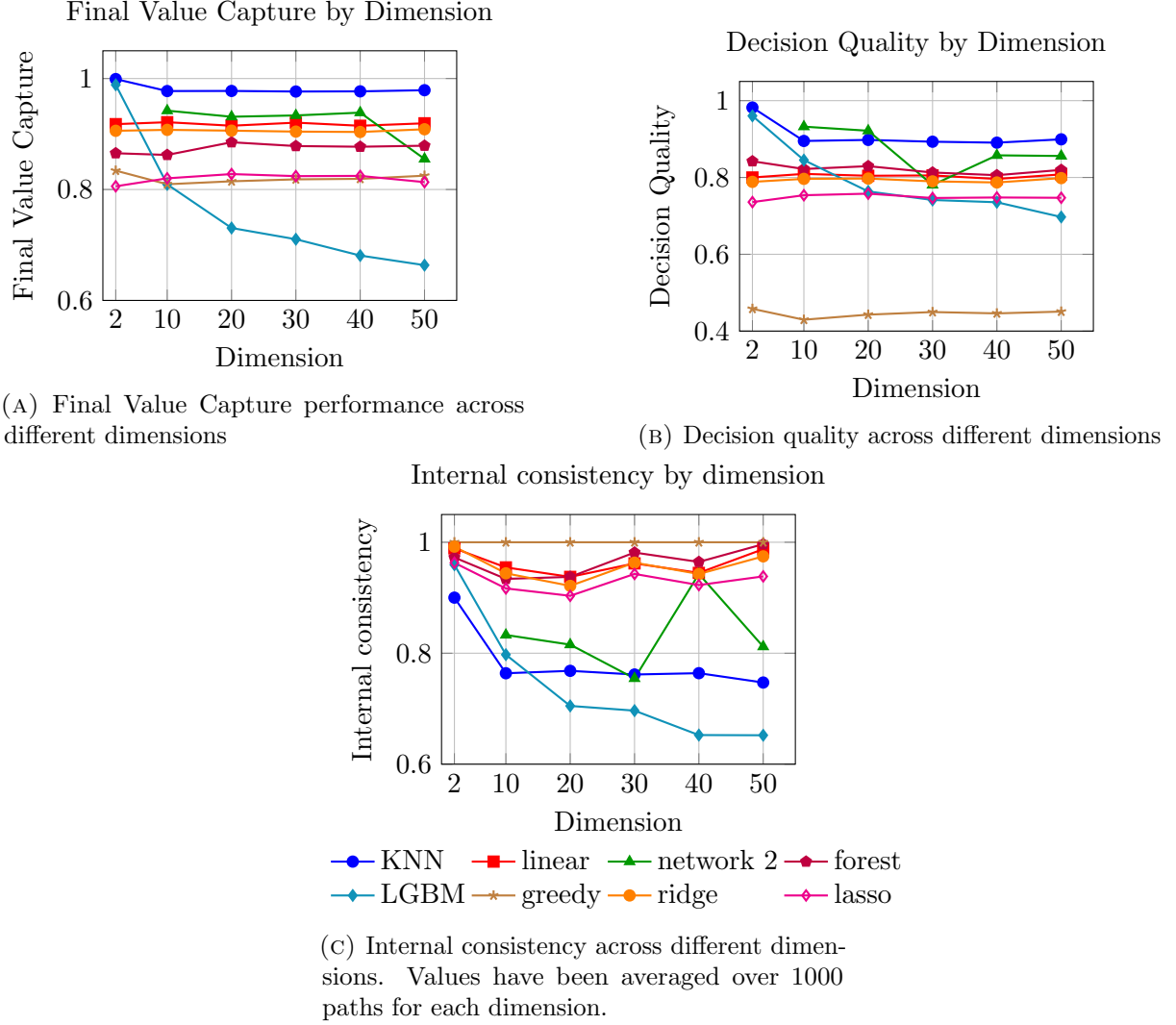


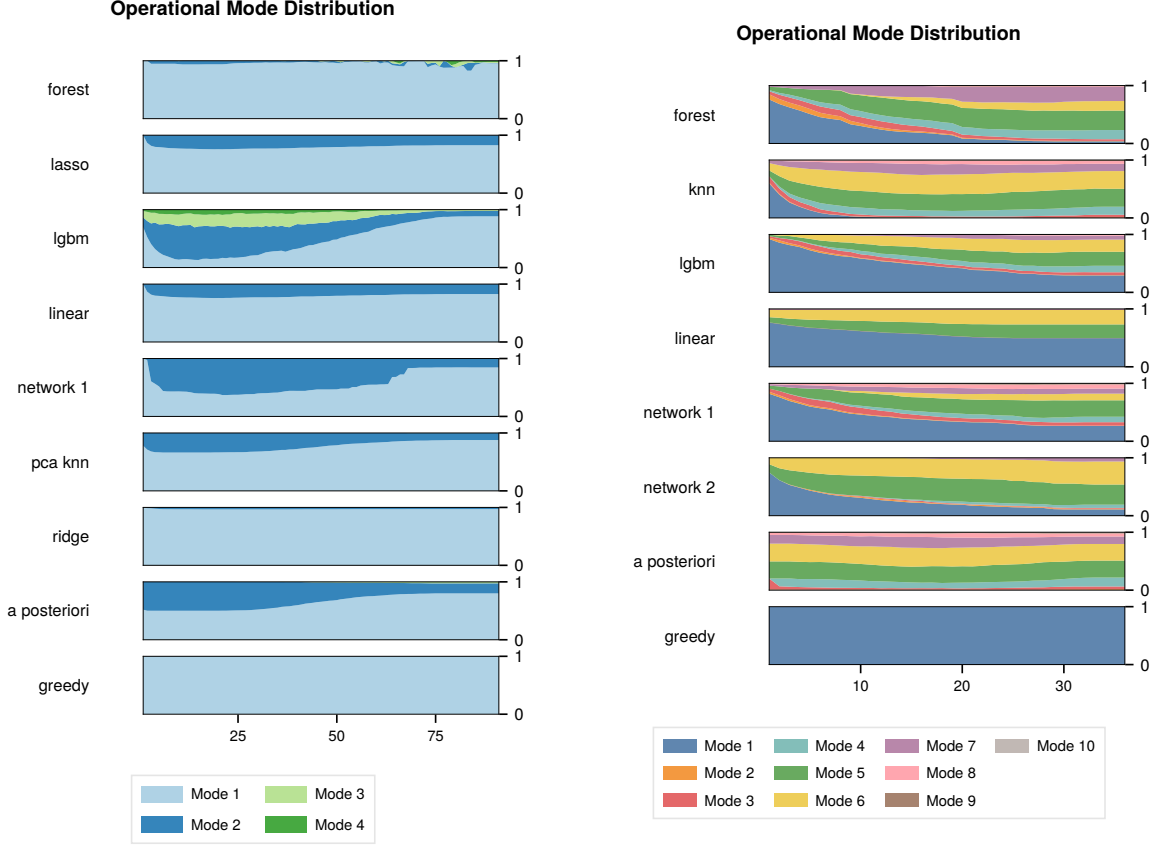
FIGURE 3. This plot shows how our three measures scale with dimension in example Section 6.4 when starting in state 1. Note that for $d > 2$, k -NN is actually PCA- k -NN.

complexity of previous approximations – methods with high variance or training instability can create erratic target functions \tilde{V}_i , potentially explaining why k -NN’s more stable local averaging maintains better decision boundaries through the backward induction.

8.2. Theoretical guarantees for k -NN Regression. Our theoretical analysis provides context for the strong empirical performance of k -NN. The concentration bounds in Theorems 5.3, 5.4 and 5.6 establish that k -NN predictions concentrate around the target \tilde{V}_i , at each regression step. This aligns with our empirical findings that k -NN identified high-quality decision boundaries in our experiments.

8.3. Limitations. Our evaluation used minimal hyperparameter tuning to assess out-of-the-box performance of classical regression models. While systematic optimization might alter relative rankings, this reflects realistic constraints for practitioners who cannot afford extensive tuning.

Our high-dimensional experiments relied on PCA for dimensionality reduction. This choice was not systematically compared against alternatives like t-SNE, UMAP, or kernel PCA, limiting conclusions about the optimal preprocessing approach. However, the strong performance of



(A) Comparison of switching strategies

(B) Comparison of switching strategies

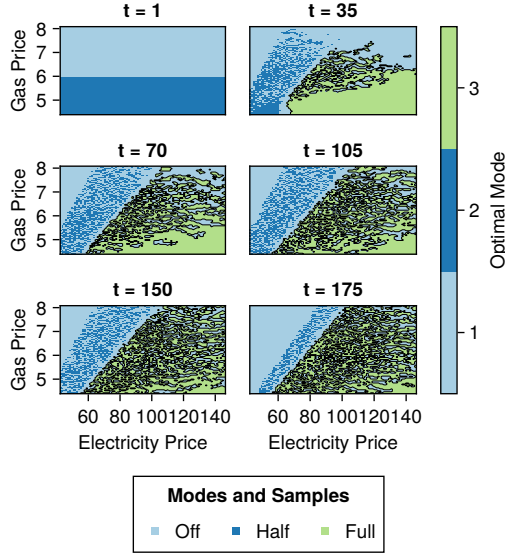
FIGURE 4. Analysis of switching strategies for OS problems. We have simulated 1000 paths and applied the strategies defined by $\mu^{\mathcal{R}}$ for each path and model when starting in state 1, and then calculated the distribution the strategies have over the different modes, over time. Left: ACLP performance. Right: BSP

PCA- k -NN suggests that dimensionality reduction can make k -NN competitive even when raw k -NN suffers from the curse of dimensionality.

8.4. Implications for regression-based solutions to optimal switching. Our results demonstrate that simple, classical methods often suffice for OS problems. In experiments, k -NN, linear models, and tree-based approaches collectively achieved near-optimal performance with greater robustness and fewer training failures than neural networks. This suggests that practitioners should exhaust the toolkit of classical regression methods before investing in neural network architectures that potentially offer minimal performance gains at significant computational and tuning costs.

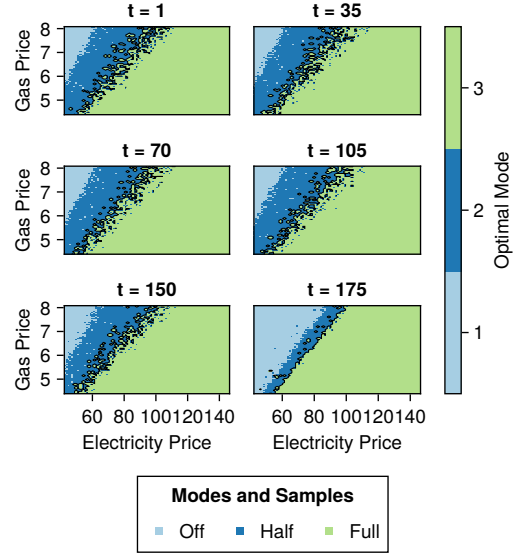
8.5. Future work. Our theoretical analysis opens several promising directions for future research. First, extending our single-step concentration bounds to characterize error propagation through full backward induction would provide a more complete theoretical understanding of the Longstaff-Schwartz algorithm. Second, our concentration bound requires sub-Gaussian or sub-exponential processes, which limits applicability to jump processes with polynomial tails. Extending the bound to these cases would broaden the scope of the method. Third, while our main theorem requires large m_Y for concentration, our experiments suggest $m_Y = 1$ is sufficient in practice, indicating that the bound likely could be tightened.

Switching Boundaries Evolution knn



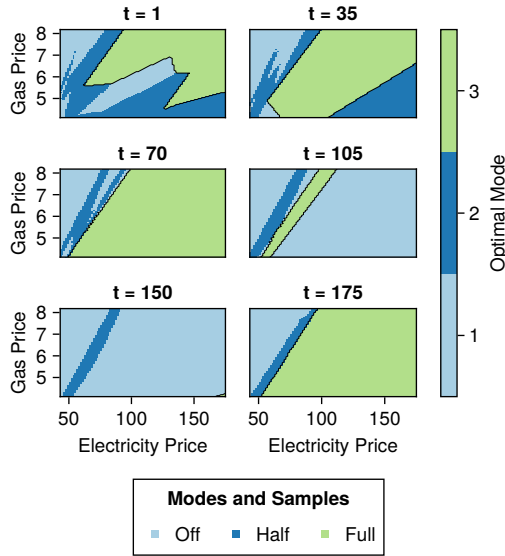
(A) k -NN Switching Boundaries

Switching Boundaries Evolution a posteriori



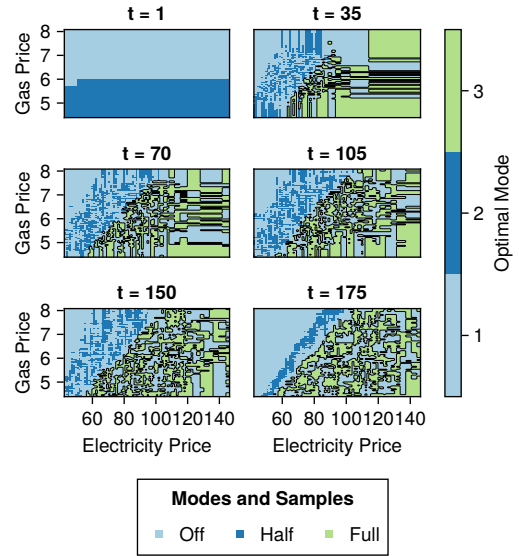
(B) A Posteriori Switching Boundaries

Switching Boundaries Evolution network 1



(C) Network Switching Boundaries

Switching Boundaries Evolution lgbm



(D) LGBM Switching Boundaries

FIGURE 5. Evolution of Switching Boundaries Using Different Regression Methods. These show the decision boundaries at different time points, when the current mode is 1 (Off) for the CL example Section 6.1. The black part shows in particular the boundary between mode 2 and mode 3.

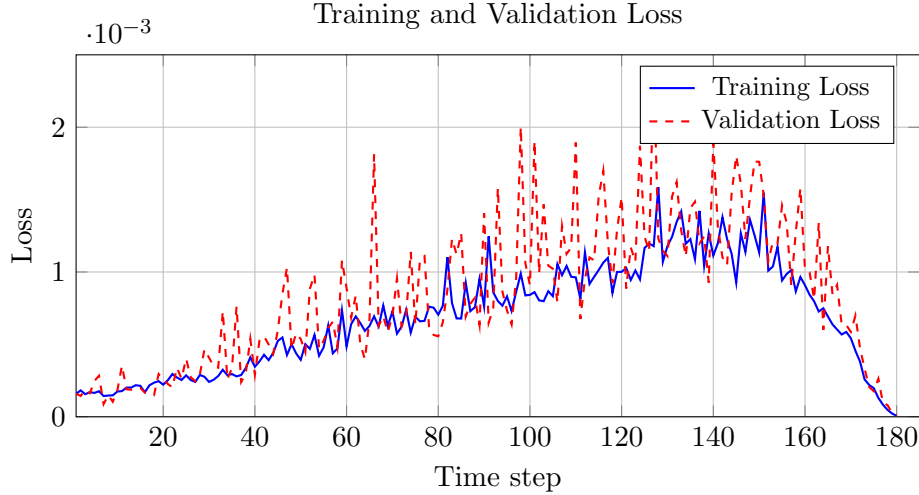


FIGURE 6. Training and validation loss curves for CL ($d = 30$) of the model PCA- k -NN. We see the average training and validation loss over modes $j = 1, 2, 3$, from time-step 1 to 180. We can see that both losses at the start of training, rightmost of figure, begin by rising. Then around time-step 140, losses start to decline.

The prediction discrepancy we observed with k -NN suggests exploring adaptive approaches. Since regression difficulty varies over time steps (see Fig. 6), hyperparameters could be dynamically adjusted, or different models could be used entirely at different time steps. Our preliminary tests with k -NN/linear model mixtures showed promise: good decision boundaries from k -NN together with better extrapolation from linear components.

Our approach treats each (time, mode)-pair as an independent regression problem, with only warm-start initialization from previous modes providing continuity in network training. Neural networks could exploit structural relationships more extensively through parameter sharing, for instance, using shared hidden layers with mode-specific output heads, or incorporating time as an input feature rather than training separate models. While our warm-starts capture some temporal continuity, joint architectures could better leverage the relationships between modes and time steps.

ACKNOWLEDGMENTS

The first author was supported by the Wallenberg AI, Autonomous Systems and Software Program (WASP) funded by the Knut and Alice Wallenberg Foundation. The second author was partially supported by the Swedish Research Council grant dnr: 2019-04098.

REFERENCES

- [ACLP14] R. Aïd, L. Campi, N. Langrené, and H. Pham. A probabilistic numerical method for optimal multiple switching problems in high dimension. *SIAM Journal on Financial Mathematics*, 5:191–231, 2014.
- [And25] M. Andersson. Numerical methods for optimal switching problems. <https://github.com/MartinDAndersson/optimal-switching-regression>, 2025. Commit d491951, accessed Jun 18, 2025.
- [BCJ19] S. Becker, P. Cheridito, and A. Jentzen. Deep optimal stopping. *Journal of Machine Learning*, 20:1–25, 2019.
- [BCJ21] S. Becker, P. Cheridito, and A. Jentzen. Solving high-dimensional optimal stopping problems using deep learning. *European Journal of Applied Mathematics*, 32:470–514, 2021.
- [BCN23] E. Bayraktar, A. Cohen, and A. Nellis. A neural network approach to high-dimensional optimal switching problems with jumps in energy markets. *SIAM Journal on Financial Mathematics*, 14(4):1028–1061, 2023.
- [BEKS17] J. Bezanson, A. Edelman, S. Karpinski, and V. Shah. Julia: A fresh approach to numerical computing. *SIAM review*, 59(1):65–98, 2017.

- [BG97] M. Broadie and P. Glasserman. Pricing american-style securities using simulation. *Journal of Economic Dynamics & Control*, 21:1323–1352, 1997.
- [BGC17] Y. Bengio, I. Goodfellow, and A. Courville. *Deep learning*, volume 1. MIT press Cambridge, MA, USA, 2017.
- [BGSS22] R. Barkhudaryan, D. Gomes, H. Shahgholian, and M. Salehi. System of variational inequalities with interconnected obstacles. *Applicable Analysis*, 101(2):605–628, 2022.
- [BHRS23] C. Bayer, P. Hager, S. Riedel, and J. Schoenmakers. Optimal stopping with signatures. *The Annals of Applied Probability*, 33(1):238–273, 2023.
- [BJK10] I. Biswas, E. Jakobsen, and K. Karlsen. Viscosity solutions for a system of integro-pdes and connections to optimal switching and control of jump-diffusion processes. *Applied mathematics and optimization*, 62:47–80, 2010.
- [BKL⁺20] A.D. Blaom, F. Kiraly, T. Lienart, Y. Simillides, D. Arenas, and S.J. Vollmer. MLJ: A julia package for composable machine learning. *Journal of Open Source Software*, 5(55):2704, 2020.
- [BLM13] S. Boucheron, G. Lugosi, and P. Massart. *Concentration inequalities*. Oxford University Press, Oxford, 2013. A nonasymptotic theory of independence, With a foreword by Michel Ledoux.
- [BØ94] K. A. Brekke and B. Øksendal. Optimal switching in an economic activity under uncertainty. *SIAM Journal on Control and Optimization*, 32:1021–1036, 1994.
- [Bre01] L. Breiman. Random forests. *Machine learning*, 45:5–32, 2001.
- [BS85] M. J. Brennan and E. S. Schwartz. Evaluating natural resource investments. *Journal of Business*, 58(2):135–157, 1985.
- [Car96] J.F. Carriere. Valuation of the early-exercise price for options using simulations and nonparametric regression. *Insurance: mathematics and Economics*, 19:19–30, 1996.
- [CH67] T. Cover and P. Hart. Nearest neighbor pattern classification. *IEEE transactions on information theory*, 13(1):21–27, 1967.
- [CIL92] M.G. Crandall, H. Ishii, and P-L. Lions. User’s guide to viscosity solutions of second-order partial differential equations. *Bulletin of the American Mathematical Society*, 27:1–67, 1992.
- [CL08] R. Carmona and M. Ludkovski. Pricing asset scheduling flexibility using optimal switching. *Applied Mathematical Finance*, 15(5-6):405–447, 2008.
- [CL10] R. Carmona and M. Ludkovski. Valuation of energy storage: An optimal switching approach. *Quantitative Finance*, 10:359–374, 2010.
- [Cyb89] G. Cybenko. Approximation by superpositions of a sigmoidal function. *Mathematics of control, signals and systems*, 2(4):303–314, 1989.
- [DHP09] B. Djehiche, S. Hamadene, and A. Popier. A finite horizon optimal multiple switching problem. *SIAM Journal on Control and Optimization*, 48(4):2751–2770, 2009.
- [EAF17] B. El Asri and I. Fakhouri. Viscosity solutions for a system of pdes and optimal switching. *IMA Journal of Mathematical Control and Information*, 34(3):937–960, 2017.
- [EAH09] B. El Asri and S. Hamadene. The finite horizon optimal multi-modes switching problem: the viscosity solution approach. *Applied Mathematics and Optimization*, 60:213–235, 2009.
- [EKPQ97] N. El-Karoui, S. Peng, and M.C. Quenez. Backward stochastic differential equations in finance. *Mathematical finance*, 7:1–71, 1997.
- [EM21] J. Ery and L. Michel. Solving optimal stopping problems with deep q-learning. *arXiv preprint*, 2021. arXiv:2101.09682.
- [ETR⁺21] S. Elsayed, D. Thyssens, A. Rashed, H. Jomaa, and L. Schmidt-Thieme. Do we really need deep learning models for time series forecasting? *arXiv preprint arXiv:2101.02118*, 2021.
- [FD21] A. Fathan and E. Delage. Deep reinforcement learning for optimal stopping with application in financial engineering. *arXiv preprint*, 2021. arXiv:2105.08877.
- [FDCBA14] M. Fernández-Delgado, E. Cernadas, S. Barro, and D. Amorim. Do we need hundreds of classifiers to solve real world classification problems? *The journal of machine learning research*, 15(1):3133–3181, 2014.
- [FDCJ19] M. Ferrari Dacrema, P. Cremonesi, and D. Jannach. Are we really making much progress? a worrying analysis of recent neural recommendation approaches. In *Proceedings of the 13th ACM conference on recommender systems*, pages 101–109, 2019.
- [Fri01] J.H Friedman. Greedy function approximation: a gradient boosting machine. *Annals of statistics*, pages 1189–1232, 2001.
- [GPP22] A. Gnoatto, M. Patacca, and A. Picarelli. A deep solver for bsdes with jumps. *arXiv preprint arXiv:2211.04349*, 2022.
- [HJW18] J. Han, A. Jentzen, and E. Weinan. Solving high-dimensional partial differential equations using deep learning. *Proceedings of the National Academy of Sciences*, 115:8505–8510, 2018.
- [HK70] A.E. Hoerl and R.W. Kennard. Ridge regression: Biased estimation for nonorthogonal problems. *Technometrics*, 12(1):55–67, 1970.
- [HK04] M.B. Haugh and L. Kogan. Pricing american options: a duality approach. *Operations Research*, 52:258–270, 2004.

- [HKRT24] C. Herrera, F. Krach, P. Ruyssen, and J. Teichmann. Optimal stopping via randomized neural networks. *Frontiers of Mathematical Finance*, 3(1):31–77, 2024.
- [HM13] S. Hamadene and M.A. Morlais. Viscosity solutions of systems of pdes with interconnected obstacles and switching problem. *Applied Mathematics & Optimization*, 67:163–196, 2013.
- [HMM19] S. Hamadene, R. Martyr, and J. Moriarty. A probabilistic verification theorem for the finite horizon two-player zero-sum optimal switching games in continuous time. *Advances in Applied Probability*, 51:425–442, 2019.
- [HPW19] C. Huré, H. Pham, and X. Warin. Some machine learning schemes for high-dimensional nonlinear pdes. *arXiv preprint arXiv:1902.01599*, 33(6):27, 2019.
- [HSW89] K. Hornik, M. Stinchcombe, and H. White. Multilayer feedforward networks are universal approximators. *Neural networks*, 2(5):359–366, 1989.
- [HT10] Y. Hu and S. Tang. Multi-dimensional bsde with oblique reflection and optimal switching. *Probability theory and related fields*, 147:89–121, 2010.
- [Hu20] R. Hu. Deep learning for ranking response surfaces with applications to optimal stopping problems. *Quantitative Finance*, 20:1567–1581, 2020.
- [KB14] D. P Kingma and J. Ba. Adam: A method for stochastic optimization. *arXiv preprint arXiv:1412.6980*, 2014.
- [Kha16] I. Kharroubi. Optimal switching in finite horizon under state constraints. *SIAM Journal on Control and Optimization*, 54:2202–2233, 2016.
- [KHNT22] A. Kohatsu-Higa, E. Nualart, and N. Tran. Density estimates for jump diffusion processes. *Applied Mathematics and Computation*, 420:126814, 2022.
- [KKT10] M. Kohler, A. Krzyzak, and N. Todorovic. Pricing of high-dimensional american options by neural networks. *Mathematical Finance*, 20:383–410, 2010.
- [KMF⁺17] G. Ke, Q. Meng, T. Finley, T. Wang, W. Chen, W. Ma, Q. Ye, and T. Liu. Lightgbm: A highly efficient gradient boosting decision tree. *Advances in neural information processing systems*, 30, 2017.
- [Led06] M. Ledoux. Concentration of measure and logarithmic sobolev inequalities. In *Seminaire de probabilités XXXIII*, pages 120–216. Springer, 2006.
- [LNO14a] N. LP Lundström, K. Nyström, and M. Olofsson. Systems of variational inequalities for non-local operators related to optimal switching problems: existence and uniqueness. *Manuscripta mathematica*, 145:407–432, 2014.
- [LNO14b] N. LP Lundström, K. Nyström, and M. Olofsson. Systems of variational inequalities in the context of optimal switching problems and operators of kolmogorov type. *Annali di Matematica Pura ed Applicata (1923-)*, 193(4):1213–1247, 2014.
- [LNO15] K. Li, K. Nyström, and M. Olofsson. Optimal switching problems under partial information. *Monte Carlo Methods and Applications*, 21:91–120, 2015.
- [LO22] N. LP Lundström and M. Olofsson. Systems of fully nonlinear parabolic obstacle problems with neumann boundary conditions. *Applied Mathematics & Optimization*, 86(2):27, 2022.
- [LOO21] N.L.P. Lundström, M. Olofsson, and T. Önskog. Management strategies for run-of-river hydropower plants: an optimal switching approach. *Optimization and Engineering*, pages 1–25, 2021.
- [LS01] F.A. Longstaff and E.S. Schwartz. Valuing american options by simulation: a simple least-squares approach. *The Review of Financial Studies*, 14:113–147, 2001.
- [Mar16] R. Martyr. Dynamic programming for discrete-time finite-horizon optimal switching problems with negative switching costs. *Advances in Applied Probability*, 48(3):832–847, 2016.
- [Mic16] Microsoft Corporation. Lightgbm, 2016. GitHub repository.
- [Olo18] M. Olofsson. A brownian optimal switching problem under incomplete information. *Electronic Communications in Probability*, 23:1–12, 2018.
- [PAG⁺24] J. Pere, B. Avelin, V. Garino, P. Ilmonen, and L. Viitasaari. On the impact of approximation errors on extreme quantile estimation with applications to functional data analysis. *arXiv preprint arXiv:2307.03581*, 2024.
- [Pal23] A. Pal. Lux: Explicit Parameterization of Deep Neural Networks in Julia, April 2023. If you use this software, please cite it as below.
- [Per18] M. Perninge. A limited-feedback approximation scheme for optimal switching problems with execution delays. *Mathematical Methods of Operations Research*, 87(3):347–382, 2018.
- [Per20] M. Perninge. A finite horizon optimal switching problem with memory and application to controlled sddes. *Mathematical Methods of Operations Research*, 91(3):465–500, 2020.
- [Per21] M. Perninge. On the finite horizon optimal switching problem with random lag. *Applied Mathematics & Optimization*, 84:355–397, 2021.
- [PP90] E. Pardoux and S. Peng. Adapted solutions of a backward stochastic differential equation. *Systems & Control Letters*, 14:55–61, 1990.
- [PP92] E. Pardoux and S. Peng. Backward stochastic differential equations and quasilinear parabolic differential equations. *Stochastic partial differential equations and their applications*, pages 200–217, 1992.

- [PS06] G. Peskir and A. Shiryaev. *Optimal stopping and free-boundary problems*. Birkhäuser, Basel, 2006.
- [Pum23] PumasAI. Simplechains.jl: Simple and fast neural networks on cpu, 2023.
- [Rog02] L.C. Rogers. Monte carlo valuation of american options. *Mathematical Finance*, 12:271–286, 2002.
- [SCS⁺22] B. Sadeghi, P. Chiarawongse, K. Squire, D.C. Jones, A. Noack, C. St-Jean, R. Huijzer, R. Schätzle, I. Butterworth, Y. Peng, and A. Blaom. DecisionTree.jl - A Julia implementation of the CART Decision Tree and Random Forest algorithms, November 2022.
- [SWL⁺16] R.P. Sheridan, W. Wang, A. Liaw, J. Ma, and E. Gifford. Extreme gradient boosting as a method for quantitative structure–activity relationships. *Journal of chemical information and modeling*, 56(12):2353–2360, 2016.
- [Tib96] R. Tibshirani. Regression shrinkage and selection via the lasso. *Journal of the Royal Statistical Society Series B: Statistical Methodology*, 58(1):267–288, 1996.
- [Til93] J.A. Tilley. Valuing american options in a path simulation model. *Transaction of the Society of Actuaries*, 1993.
- [TVR99] J.N. Tsitsiklis and B. Van Roy. Optimal stopping of markov processes: Hilbert space theory, approximation algorithms, and an application to pricing high-dimensional financial derivatives. *IEEE Transactions on Automatic Control*, 44:1840–1851, 1999.
- [TY93] S. Tang and J. Yong. Finite horizon stochastic optimal switching and impulse controls with a viscosity solution approach. *Stochastics: An International Journal of Probability and Stochastic Processes*, 45(3-4):145–176, 1993.

APPENDIX A. ADDITIONAL TABLES

This section contains tables for the plots in Fig. 2.

TABLE 6. Performance Metrics of Different Strategies, CL Experiment

Strategy	Final Value Capture	Decision Quality	Internal Consistency
k -NN	0.9911	0.9505	0.9742
LGBM	0.9905	0.9436	0.9987
Network 1	0.9748	0.9172	0.9752
Forest	0.9025	0.8053	0.9685
Linear	0.8984	0.7951	0.9821
Greedy	0.2466	0.0731	1.0000

Note: Bold values indicate the best performance in each metric category.

TABLE 7. Performance Metrics of Different Strategies, ACLP Experiment

Strategy	Final Value Capture	Decision Quality	Internal Consistency
LASSO	0.9939	0.6869	0.9775
Linear	0.9938	0.6851	0.9853
Ridge	0.9938	0.6652	0.9903
Network 1	0.9937	0.7175	0.9315
Greedy	0.9932	0.6505	1.0000
PCA k -NN	0.9919	0.6494	0.9795
Forest	0.9813	0.6415	0.9731
LGBM	0.9343	0.5871	0.9028

Note: Bold values indicate the best performance in each metric category.

TABLE 8. Performance Metrics of Different Strategies, BSP Experiment

Strategy	Final Value Capture	Decision Quality	Internal Consistency
k -NN	0.7744	0.7381	0.7777
Network 2	0.4962	0.4420	0.5560
Network 1	0.3788	0.3578	0.4768
Forest	0.3489	0.3298	0.4840
LGBM	0.3398	0.3326	0.3439
Linear	0.0979	0.1042	0.2250
Greedy	0.0050	0.0030	1.0000

Note: Bold values indicate the best performance in each metric category.

TABLE 9. Performance Metrics of Different Strategies, HCL Dimension = 50

Strategy	Final Value Capture	Decision Quality	Internal Consistency
k -NN	0.9769	0.8944	0.7845
Linear	0.9118	0.8044	0.8953
Ridge	0.9026	0.7969	0.8849
Forest	0.8983	0.8289	0.9374
Network 2	0.8763	0.8593	0.7605
LASSO	0.8397	0.7662	0.8856
Greedy	0.8084	0.4470	1.0000
LGBM	0.6436	0.6937	0.5781

Note: Bold values indicate the best performance in each metric category.

APPENDIX B. IMPLEMENTATION DETAILS

For a link to the code for our experiments, see [And25]. The repository includes core implementations of the simulation environments and scripts to run each experiment in Section 6. While full reproduction requires some manual configuration, we provide documentation to guide the process and code to generate all figures.

B.1. Software and Packages. All models except neural networks use MLJ.jl [BKL⁺20] in Julia [BEKS17]. Specific packages:

- Random Forests: `DecisionTrees.jl` [SCS⁺22]
- LightGBM: `LightGBM.jl` wrapper around [Mic16]
- k-NN: `NearestNeighbor.jl`
- Neural Networks: `SimpleChains.jl` [Pum23] through `Lux.jl` [Pal23] interface (optimized for small CPU models, eliminating GPU transfer overhead for NxD model training)

B.2. Model Configurations. Table 10 gives an overview of hyperparameters used in simulations.

TABLE 10. Machine Learning Models and Parameters

Model	Parameters
k -NN*	$k = 10$
PCA- k -NN*	PCA dimensions = 6, $k = 10$
Random Forest	Trees = 25, Max depth = 3
LightGBM	Iterations = 200, Learning rate = 0.05, Leaves = 31, Min data in leaf = 100, $\lambda_{L2} = 0.5$, Bagging fraction = 0.8
Ridge Regression*	$\lambda = 0.1$
Lasso Regression*	$\lambda = 0.1$
Linear Regression*	Order = $\begin{cases} 6 & \text{if } d = 2 \\ 1 & \text{otherwise} \end{cases}$
Neural Networks	See Appendix B.3

*Model is precomposed with standardization of input features

B.3. Neural Network Architecture Exploration and Final Configurations.

Exploration process. We tested the following variations:

- **Activations:** ReLU, Tanh
- **Architecture:** 1-4 hidden layers, widths up to 256 units, including pyramid shapes
- **Regularization:** With/without dropout (rates 0.1-0.3 when used)
- **Training:** Various optimizer parameters, with/without early stopping
- **Initialization:** Including the backward initialization scheme described in Section 5

The reported architectures achieved the best and most stable performance across these variations.

Final architectures.

We use architectures that vary capacity and depth:

All architectures use:

- ReLU activation for hidden layers
- Linear activation for output layer
- Dropout rate 0.1 after each hidden layer
- ADAM optimizer with exponential learning rate decay

Architecture selection: Low-capacity networks for experiments in Sections 6.1 and 6.3. High-capacity networks for higher-dimensional problems in Sections 6.2 and 6.4.

TABLE 11. Neural Network Architectures

Architecture	Layers	Usage
Low Shallow	Input \rightarrow Dense(32) \rightarrow Output	Low-dimensional experiments
Low Deep	Input \rightarrow Dense(32) \rightarrow Dense(16) \rightarrow Output	Low-dimensional experiments
High Shallow	Input \rightarrow Dense(128) \rightarrow Output	High-dimensional experiments
High Deep	Input \rightarrow Dense(128) \rightarrow Dense(64) \rightarrow Output	High-dimensional experiments

B.4. Computational Environment. All simulations were conducted on a system with the following specifications:

- **Processor:** AMD Ryzen Threadripper 1920X (12 cores, 24 threads, 3.5 GHz max frequency)
- **Memory:** 64 GB RAM
- **Operating System:** Ubuntu 20.04.6 LTS
- **Kernel:** Linux 5.15.0-105-generic
- **Architecture:** x86_64

APPENDIX C. PROOF OF THEOREM 5.3

We will break down the proof of Theorem 5.3 into several lemmas, each one dealing with a different piece of the error estimate of $\tilde{V}_i(t_n, x)$ with respect to $\hat{V}_i(t_n, x)$. We start with the growth and Lipschitz regularity of $\tilde{V}_i(t_n, x)$.

Lemma C.1. *Consider the function $\tilde{V}_i(t_n, x)$, as defined in (5.3), and assume the conditions as in Theorem 5.3. Then there exists a constant $C_0(d, L, \lambda_1, \lambda_2)$ such that*

$$|\tilde{V}_i(t_n, x)| + |\nabla_x \tilde{V}_i(t_n, x)| \leq C_0(\|x\| + 1).$$

Proof. If we denote

$$g(x, y) = \max_j (\Delta_t f_j(t_n, x) - c_{ij}(t_n, x) + \hat{V}_j(t_{n+1}, y))$$

then we can write

$$\nabla_x \tilde{V}_i(t_n, x) = \int \nabla_x \rho(x, t_n; y, t_{n+1}) g(x, y) dy.$$

Now from the growth bounds on f_j , c_{ij} and \hat{V}_j together with (5.2) and a change of variables we get that there exists constants C (not necessarily the same at every line) and $\lambda > 0$ such that

$$\begin{aligned} |\nabla_x \tilde{V}_i(t_n, x)| &\leq C \int \|\nabla_x \rho(x, t_n; y, t_{n+1})\| (\|x\| + \|y\| + 1) dy \\ &\leq C \int (\|z + x\| + 1) \exp(-\lambda \|z\|^2/t) dz \leq C(\|x\| + 1). \end{aligned}$$

A similar calculation shows that $|\tilde{V}_i(t_n, x)| \leq C(\|x\| + 1)$. \square

Using (5.3)–(5.5) we define the conditional expected estimator as

$$\widetilde{\tilde{V}}_i(t_n, x) = \mathbb{E} \left[\hat{V}_i(t_n, x) \middle| D_T \right] = \frac{1}{k} \sum_{s \in \mathcal{N}_{t_n}(x)} \tilde{V}_i(t_n, X_{t_n}^s), \quad (\text{C.1})$$

where $\mathcal{N}_{t_n}(x)$ is the set of k -nearest neighbors of x out of the set D_T at time t_n with respect to the Euclidean distance.

Before we proceed let us state a well known lemma about sub-Gaussian random variables.

Definition C.2. A random variable X is sub-Gaussian with variance proxy $\sigma^2 > 0$ if for all $s \in \mathbb{R}$ we have

$$\mathbb{E}[e^{s(X - \mathbb{E}[X])}] \leq e^{\frac{s^2 \sigma^2}{2}}. \quad (\text{C.2})$$

Lemma C.3. Let X_1, \dots, X_n be independent sub-Gaussian random variables with variance proxy $\sigma^2 > 0$. Then for any $\delta > 0$ we have

$$\mathbb{P}(|\bar{X}_n - \mathbb{E}[\bar{X}_n]| \geq \delta) \leq 2e^{-\frac{n\delta^2}{2\sigma^2}},$$

where $\bar{X}_n = \frac{1}{n} \sum_{i=1}^n X_i$.

The following lemma controls the stochastic error of the one-step forward estimate and does not depend on the specific structure of D_T .

Lemma C.4. Consider the functions $\hat{V}_i(t_n, x)$ and $\bar{V}_i(t_n, x)$ as defined in (5.4) and (C.1), and assume the conditions as in Theorem 5.3. Then there exists $\sigma(L, \lambda_1) > 0$ such that for any $\delta > 0$ we have

$$\mathbb{P}\left(\sup_x |\hat{V}_i(t_n, x) - \bar{V}_i(t_n, x)| \geq \delta \mid D_T\right) \leq \binom{M}{k} \exp\left(-\frac{km_Y\delta^2}{2\sigma^2}\right).$$

Proof. Let $E_1(x) = \hat{V}_i(t_n, x) - \bar{V}_i(t_n, x)$, then we can write

$$E_1(x) = \frac{1}{k} \sum_{s \in \mathcal{N}_{t_n}(x)} \left(\hat{V}_i(t_n, x) - \bar{V}_i(t_n, X_{t_n}^s) \right) =: \frac{1}{km_Y} \sum_{s \in \mathcal{N}_{t_n}(x)} \sum_{\hat{s}=1}^{m_Y} \varepsilon_{(s, \hat{s})},$$

where each term $\varepsilon_{(s, \hat{s})}$ is independent and is sub-Gaussian with variance proxy $\sigma^2(\lambda_1, L) > 0$. This follows from the growth assumptions on f_j , c_{ij} and $\hat{V}_j(t_{n+1}, x)$ together with (5.2).

Now define $l_i(x) = \frac{1_{\mathcal{N}_{t_n}(x)}(i)}{k}$ and define the vectors $\mathbf{l}(x) = (l_1(x), \dots, l_m(x))$ and $\boldsymbol{\varepsilon} = (\frac{1}{m_Y} \sum_{\hat{s}=1}^{m_Y} \varepsilon_{(1, \hat{s})}, \dots, \frac{1}{m_Y} \sum_{\hat{s}=1}^{m_Y} \varepsilon_{(M, \hat{s})})$, then we have

$$\sup_x |E_1(x)| = \sup_x |\mathbf{l}(x) \cdot \boldsymbol{\varepsilon}| \leq \sup_{\boldsymbol{\theta} \in P} \boldsymbol{\theta} \cdot \boldsymbol{\varepsilon},$$

where P is the convex polytope $\{\boldsymbol{\theta} \in \mathbb{R}^M; \sum_{i=1}^M |\theta_i| \leq 1, \max_i |\theta_i| \leq 1/k\}$. We note that at each corner $\boldsymbol{\theta}$ of P (the set of which we call P_V) we have that $\boldsymbol{\theta} \cdot \boldsymbol{\varepsilon}$ is sub-Gaussian with variance proxy $(\sigma^2/(m_Y k))$, since by independence of $\varepsilon_{(i, j)}$ we have for any $\lambda \in \mathbb{R}$

$$\begin{aligned} \mathbb{E}[e^{\lambda \boldsymbol{\theta} \cdot \boldsymbol{\varepsilon}}] &= \prod_{i=1}^M \mathbb{E}[e^{\lambda \theta_i \frac{1}{m_Y} \sum_{j=1}^{m_Y} \varepsilon_{(i, j)}}] \leq \prod_{i=1}^M \prod_{j=1}^{m_Y} e^{\frac{\lambda^2 \theta_i^2 \sigma^2}{2m_Y^2}} \leq e^{\frac{\lambda^2 (\sum_{i=1}^M \theta_i^2) \sigma^2}{2m_Y}} \\ &\leq e^{\frac{\lambda^2 \sigma^2}{2km_Y}}. \end{aligned} \tag{C.3}$$

Now, a linear function inside a convex polytope achieves its maximum at one of the vertices of the polytope, as such we can use the union bound, (C.3) and Lemma C.3 to get

$$\mathbb{P}(\sup_x |E_1(x)| \geq \delta) \leq \sum_{\boldsymbol{\theta} \in P_V} \mathbb{P}(\boldsymbol{\theta} \cdot \boldsymbol{\varepsilon} \geq \delta) \leq \binom{M}{k} \exp\left(-\frac{km_Y\delta^2}{2\sigma^2}\right).$$

□

Under some additional assumptions, like assuming that $\log(\varrho(x, t; y, t + \Delta t))$ is concave w.r.t. y we can obtain an alternative bound. That is, if we consider the function $\sup_{\boldsymbol{\theta} \in P} \boldsymbol{\theta} \cdot \boldsymbol{\varepsilon}$, we first note that it is a Lipschitz function w.r.t. $\boldsymbol{\varepsilon}$ with Lipschitz constant $1/k$, i.e.

$$|\sup_{\boldsymbol{\theta} \in P} \boldsymbol{\theta} \cdot \boldsymbol{\varepsilon}_1 - \sup_{\boldsymbol{\theta} \in P} \boldsymbol{\theta} \cdot \boldsymbol{\varepsilon}_2| \leq \sup_{\boldsymbol{\theta} \in P} \|\boldsymbol{\theta}\| \|\boldsymbol{\varepsilon}_1 - \boldsymbol{\varepsilon}_2\|$$

where $\sup_{\boldsymbol{\theta} \in P} \|\boldsymbol{\theta}\| = 1/\sqrt{k}$ and is attained at one of the vertices of P . From this we get (see [Led06])

$$\begin{aligned} \mathbb{P}(\sup |E_1(x)| \geq \delta) &\leq \mathbb{P}(\sup_{\boldsymbol{\theta} \in P} \boldsymbol{\theta} \cdot \boldsymbol{\varepsilon} \geq \delta) = \mathbb{P}\left(\sup_{\boldsymbol{\theta} \in P} \boldsymbol{\theta} \cdot \boldsymbol{\varepsilon} - \mathbb{E}[\sup_{\boldsymbol{\theta} \in P} \boldsymbol{\theta} \cdot \boldsymbol{\varepsilon}] \geq \delta - \mathbb{E}[\sup_{\boldsymbol{\theta} \in P} \boldsymbol{\theta} \cdot \boldsymbol{\varepsilon}]\right) \\ &\leq \exp\left(-\frac{(\delta - \mathbb{E}[\sup_{\boldsymbol{\theta} \in P} \boldsymbol{\theta} \cdot \boldsymbol{\varepsilon}])^2 km_Y}{\sigma^2}\right). \end{aligned}$$

In the above, the term $\mathbb{E}[\sup_{\theta \in P} \theta \cdot \varepsilon]$ is a (Gaussian like) complexity measure of the convex polytope P with respect to ε . To estimate the complexity, we use Hölder's inequality and (5.2) to get that there exists a constant C such that

$$\mathbb{E}[\sup_{\theta \in P} \theta \cdot \varepsilon] \leq \mathbb{E}[\sup_{\theta \in P} \|\theta\| \|\varepsilon\|] \leq \frac{1}{\sqrt{k}} (\mathbb{E}[\|\varepsilon\|^2])^{1/2} \leq \frac{\sqrt{M}}{\sqrt{km_Y}} C.$$

Putting this together yields the estimate whenever $\delta > \frac{\sqrt{M}}{2\sqrt{km_Y}} C$, for some constant C_1 ,

$$\mathbb{P} \left(\sup_x |\widehat{V}_i(t_n, x) - \widetilde{V}_i(t_n, x)| \geq \delta \mid D_T \right) \leq \exp \left(-\frac{km_Y \delta^2}{C_1} \right).$$

In order to control the error between the average k -nearest estimate and the true value function we need the following local random error estimate. One effect, is that under our assumptions in Theorem 5.3, the error is controlled entirely by the information in D_T at time t_n , as such it “localizes” the error in time.

Lemma C.5. *Let the functions $\widetilde{V}_i(t_n, x)$ and $\widehat{V}_i(t_n, x)$ be as defined as in (5.3) and (C.1), and assume the conditions as in Theorem 5.3. Let $Q \subset \mathbb{R}^d$ be a bounded set, then there exists a constant $C(d, L, Q, \lambda_1, \lambda_2)$ such that for any $x \in Q$ we have*

$$|\widehat{V}_i(t_n, x) - \widetilde{V}_i(t_n, x)| \leq C \frac{1}{k} \sum_{s \in \mathcal{N}_{t_n}(x)} (\|X_{t_n}^s\| + 1) \|X_{t_n}^s - x\|$$

Proof. From Lemma C.1 and the definition of $\widehat{V}_i(t_n, x)$ we have

$$\begin{aligned} |\widehat{V}_i(t_n, x) - \widetilde{V}_i(t_n, x)| &\leq \frac{1}{k} \sum_{s \in \mathcal{N}_{t_n}(x)} |\widetilde{V}_i(t_n, X_{t_n}^s) - \widetilde{V}_i(t_n, x)| \\ &\leq C \frac{1}{k} \sum_{s \in \mathcal{N}_{t_n}(x)} (\|X_{t_n}^s\| + 1) \|X_{t_n}^s - x\|. \end{aligned}$$

□

Finally, we are ready to estimate the stochastic error between \widetilde{V} and \widehat{V} , this depends on the structure of the set D_T at time t_n , specifically on how likely it is to see a hole at time t_n in Q .

Lemma C.6. *Consider the functions $\widetilde{V}_i(t_n, x)$ and $\widehat{V}_i(t_n, x)$ as defined in (5.3) and (C.1), and assume the conditions as in Theorem 5.3. Then, there exists constants $C_1(d, L, Q, \lambda_1, \lambda_2)$ and $C_2(d, L, Q, \lambda_1, \lambda_2)$ such that*

$$\mathbb{P}(\sup_{x \in Q} |\widehat{V}_i(t_n, x) - \widetilde{V}_i(t_n, x)| \geq \delta) \leq \begin{cases} C_1 \frac{|Q|}{\delta^d} \exp \left(-\frac{M \left(\frac{M-k}{M} - \sup_Q p_{\delta/(4C_2)}^c \right)_+^2}{2} \right) & \text{if } \delta/C_2 \leq 1, \\ C_1 \frac{|Q|}{\delta^{d/2}} \exp \left(-\frac{M \left(\frac{M-k}{M} - \sup_Q p_{\sqrt{\delta/(4C_2)}}^c \right)_+^2}{2} \right) & \text{if } \delta/C_2 > 1, \end{cases}$$

where $p_r^c(x) = \mathbb{P}(X_{t_n}^1 \notin B_r(x))$.

Proof. We use Lemma C.5 to get the existence of a constant C_2 such that

$$\begin{aligned} \mathbb{P}(\sup_{x \in Q} |\widehat{V}_i(t_n, x) - \widetilde{V}_i(t_n, x)| \geq \delta) &\leq \mathbb{P} \left(\sup_{x \in Q} \frac{1}{k} \sum_{s \in \mathcal{N}_{t_n}(x)} (\|X_{t_n}^s\| + 1) \|X_{t_n}^s - x\| \geq \frac{\delta}{C} \right) \\ &\leq \mathbb{P} \left(\sup_{x \in Q} (U_n(x)^2 + U_n(x)) \geq \frac{\delta}{C_2} \right) \end{aligned}$$

where $U_n(x) = \max_{s \in \mathcal{N}_{t_n}(x)} \|X_{t_n}^s - x\|$. Now, depending on if $\delta/C_2 \leq 1$ the quadratic term is the dominating term or the linear term, i.e. we have

$$\mathbb{P} \left(\sup_{x \in Q} (U_n(x)^2 + U_n(x)) \geq \frac{\delta}{C_2} \right) \leq \begin{cases} \mathbb{P} \left(\sup_{x \in Q} U_n(x) \geq \frac{\delta}{2C_2} \right) & \text{if } \delta/C_2 \leq 1, \\ \mathbb{P} \left(\sup_{x \in Q} U_n(x) \geq \sqrt{\frac{\delta}{2C_2}} \right) & \text{if } \delta/C_2 > 1. \end{cases} \quad (\text{C.4})$$

Now, by letting for a set A , $\nu_M(A) = \frac{1}{M} \sum_{i=1}^M \mathbf{1}_A(X_{t_n}^i)$ be the empirical measure of the set A , and let $\nu(A) = \mathbb{P}(X_{t_n}^1 \in A)$ be the true measure. Then for any $\hat{\delta} > 0$, we have for $\mathcal{A}_{\hat{\delta}} := \{B_{\hat{\delta}}^c(x); x \in Q\}$ the following

$$\mathbb{P} \left(\sup_{x \in Q} U_n(x) \geq \hat{\delta} \right) = \mathbb{P} \left(\sup_{A \in \mathcal{A}_{\hat{\delta}}} \nu_M(A) \geq \frac{M-k}{M} \right).$$

Now, there exists a set $\mathcal{B}_{\hat{\delta}} = \{B_{\hat{\delta}/2}^c(x) : x \in P_0\}$ for some finite set of points P_0 such that for any $A \in \mathcal{A}_{\hat{\delta}}$ there is a point $x_0 \in P_0$ such that $A \subset B_{\hat{\delta}/2}^c(x_0)$. Furthermore, the set P_0 contains at most $O(|Q|/\hat{\delta}^d)$ points. We can now write by the monotonicity of the empirical measure

$$\mathbb{P} \left(\sup_{A \in \mathcal{A}_{\hat{\delta}}} \nu_M(A) \geq \frac{M-k}{M} \right) \leq \mathbb{P} \left(\max_{B \in \mathcal{B}_{\hat{\delta}}} \nu_M(B) \geq \frac{M-k}{M} \right).$$

Finally, from the triangle inequality, the union bound and Hoeffding's inequality we get

$$\begin{aligned} & \mathbb{P} \left(\max_{B \in \mathcal{B}_{\hat{\delta}}} (\nu_M(B) - \nu(B)) \geq \frac{M-k}{M} - \max_{B \in \mathcal{B}_{\hat{\delta}}} \nu(B) \right) \\ & \leq \sum_{B \in \mathcal{B}_{\hat{\delta}}} \mathbb{P} \left(\nu_M(B) - \nu(B) \geq \frac{M-k}{M} - \max_{B \in \mathcal{B}_{\hat{\delta}}} \nu(B) \right) \\ & \leq C \frac{|Q|}{\hat{\delta}^d} \exp \left(\frac{-M \left(\frac{M-k}{M} - \max_{B \in \mathcal{B}_{\hat{\delta}}} \nu(B) \right)_+^2}{2} \right). \end{aligned} \quad (\text{C.5})$$

Now, from (C.4) and (C.5) we get in the case $\delta/C_2 \leq 1$ that

$$\mathbb{P}(\sup_{x \in Q} |\widetilde{V}_i(t_n, x) - \widetilde{V}_i(t_n, x)| \geq \delta) \leq C \frac{|Q|}{\delta^d} \exp \left(\frac{-M \left(\frac{M-k}{M} - \sup_Q p_{\delta/(4C_2)}^c \right)_+^2}{2} \right),$$

and, in the case $\delta/C_2 > 1$ we get

$$\mathbb{P}(\sup_{x \in Q} |\widetilde{V}_i(t_n, x) - \widetilde{V}_i(t_n, x)| \geq \delta) \leq C \frac{|Q|}{\delta^{d/2}} \exp \left(\frac{-M \left(\frac{M-k}{M} - \sup_Q p_{\sqrt{\delta/(4C_2)}}^c \right)_+^2}{2} \right).$$

□

Remark C.7. We note that the random variable $U_n(x)$ in the proof above, is the k :th order statistic of the random variables $\|X_{t_n}^s - x\|$, and in the case the transition density is regularly varying, concentration estimates for the k :th order statistic can be found in [PAG⁺24]. This happens for instance in the case of jump-diffusion processes, where the random variable Y_i is fat tailed as in the case of the CL example in Section 6.1.

Finally, we ready to tackle the truncated version of $\widehat{\widetilde{V}}_i(t_n, x)$ defined in (5.5). This is the final piece of the puzzle in the proof of Theorem 5.3, and it says that the truncation does not introduce a large error. The reason is that $\widehat{\widetilde{V}}$ inherits with high probability the growth of \widetilde{V} , which is half the truncation level.

Lemma C.8. Consider the functions $\widehat{V}_i(t_n, x)$ and $\widetilde{V}_i(t_n, x)$ as defined in (5.4) and (5.5), and assume the conditions as in Theorem 5.3. Let the constant C_0 in (5.5) be the same as in Lemma C.1. There exists constants $C_1, C_2, \sigma > 0$, depending only on d, L, Q, λ_1 , and λ_2 , such that for any fixed bounded set $Q \subset \mathbb{R}^d$ and $\delta > 0$ we have that

$$\begin{aligned} \mathbb{P}(\sup_{x \in Q} |\widehat{V}_i(t_n, x) - \widetilde{V}_i(t_n, x)| \geq \delta) &\leq 2 \binom{M}{k} \exp\left(-\frac{km_Y(C_0 + \delta)^2}{2\sigma^2}\right) \\ &\quad + \begin{cases} C_1 \frac{|Q|}{(C_0 + \delta)^d} \exp\left(-\frac{M\left(\frac{M-k}{M} - \sup_Q p_{(C_0 + \delta)/(4C_2)}^c\right)_+^2}{2}\right) & \text{if } (C_0 + \delta)/C_2 \leq 1, \\ C_1 \frac{|Q|}{(C_0 + \delta)^{d/2}} \exp\left(-\frac{M\left(\frac{M-k}{M} - \sup_Q p_{\sqrt{(C_0 + \delta)/(4C_2)}}^c\right)_+^2}{2}\right) & \text{if } (C_0 + \delta)/C_2 > 1. \end{cases} \end{aligned}$$

Proof. By the definition of $\widehat{V}_i(t_n, x)$ we have for the constant C_0 from Lemma C.1 that

$$\mathbb{P}(\sup_{x \in Q} |\widehat{V}_i(t_n, x) - \widetilde{V}_i(t_n, x)| \geq \delta) = \mathbb{P}(\sup_{x \in Q} (\widehat{V}_i(t_n, x) - 2C_0(\|x\| + 1)) \geq \delta).$$

Now by adding and subtracting the terms $\widetilde{\widetilde{V}}_i(t_n, x)$ and $\widetilde{V}_i(t_n, x)$ we get from Lemma C.1 and the union bound that

$$\begin{aligned} \mathbb{P}\left(\sup_{x \in Q} \left[(\widehat{V}_i(t_n, x) - \widetilde{\widetilde{V}}_i(t_n, x)) + (\widetilde{\widetilde{V}}_i(t_n, x) - \widetilde{V}_i(t_n, x)) + (\widetilde{V}_i(t_n, x) - 2C_0(\|x\| + 1)) \right] \geq \delta \right) \\ \leq \mathbb{P}\left(\sup_{x \in Q} \left[(\widehat{V}_i(t_n, x) - \widetilde{\widetilde{V}}_i(t_n, x)) + (\widetilde{\widetilde{V}}_i(t_n, x) - \widetilde{V}_i(t_n, x)) \right] > C_0 + \delta \right) \\ \leq \mathbb{P}\left(\sup_{x \in Q} (\widehat{V}_i(t_n, x) - \widetilde{\widetilde{V}}_i(t_n, x)) > (C_0 + \delta)/2 \right) \\ + \mathbb{P}\left(\sup_{x \in Q} (\widetilde{\widetilde{V}}_i(t_n, x) - \widetilde{V}_i(t_n, x)) > (C_0 + \delta)/2 \right). \end{aligned}$$

The proof is complete after applying Lemmas C.4 and C.6. \square

Proof of Theorem 5.3. First note that

$$\begin{aligned} |\widehat{V}_i(t_n, x) - \widetilde{V}_i(t_n, x)| &\leq |\widehat{V}_i(t_n, x) - \widetilde{\widetilde{V}}_i(t_n, x)| + |\widetilde{\widetilde{V}}_i(t_n, x) - \widetilde{V}_i(t_n, x)| \\ &\quad + |\widehat{V}_i(t_n, x) - \widetilde{V}_i(t_n, x)| \\ &=: E_1(x) + E_2(x) + E_3(x). \end{aligned}$$

As such by the union bound

$$\begin{aligned} \mathbb{P}\left(\sup_{x \in Q} |\widehat{V}_i(t_n, x) - \widetilde{V}_i(t_n, x)| \geq \delta\right) &\leq \mathbb{P}\left(\sup_{x \in Q} E_1(x) \geq \delta/3\right) + \mathbb{P}\left(\sup_{x \in Q} E_2(x) \geq \delta/3\right) \\ &\quad + \mathbb{P}\left(\sup_{x \in Q} E_3(x) \geq \delta/3\right). \end{aligned}$$

Thus, we complete the estimate by applying Lemmas C.4, C.6 and C.8. \square

APPENDIX D. PROOF OF THEOREM 5.4

The proof of Theorem 5.4 is simpler than that of Theorem 5.3, we will modify Lemma C.4 to account for the fact that x is fixed which drastically improves the concentration of the error.

Lemma D.1. Consider the functions $\widehat{V}_i(t_n, x)$ and $\widetilde{V}_i(t_n, x)$ as defined in Section 5 and (C.1), and assume the conditions as in Theorem 5.3. Then there exists $\sigma(L, \Delta_t, \lambda_1) > 0$ such that for any $\delta > 0$ we have

$$\mathbb{P} \left(|\widehat{V}_i(t_n, x) - \widetilde{V}_i(t_n, x)| \geq \delta \mid D_T \right) \leq 2 \exp \left(-\frac{km_Y \delta^2}{2\sigma^2} \right).$$

Proof. As in the proof of Lemma C.4 we have

$$\mathbb{P} \left(|\widehat{V}_i(t_n, x) - \widetilde{V}_i(t_n, x)| \geq \delta \mid D_T \right) = \mathbb{P} (|E_1(x)| \geq \delta \mid D_T)$$

where

$$E_1(x) = \frac{1}{km_Y} \sum_{s \in \mathcal{N}_{t_n}(x)} \sum_{\hat{s}=1}^{m_Y} \varepsilon_{(s, \hat{s})}.$$

Recall that each term $\varepsilon_{(s, \hat{s})}$ is independent and is sub-Gaussian with variance proxy $\sigma^2(\lambda_1, L) > 0$. Now by Lemma C.3 and the Markov property we get that

$$\mathbb{P} (|E_1(x)| \geq \delta \mid D_T) \leq 2 \exp \left(-\frac{km_Y \delta^2}{2\sigma^2} \right).$$

□

Lemma D.2. Consider the functions $\widetilde{V}_i(t_n, x)$ and $\tilde{V}_i(t_n, x)$ as defined in Section 5 and (C.1), and assume the conditions as in Theorem 5.3. Then, there exists constants $C_1(d, \Delta t, L, |x|, \lambda_1, \lambda_2)$ and $C_2(d, \Delta t, L, |x|, \lambda_1, \lambda_2)$ such that

$$\mathbb{P} (|\widetilde{V}_i(t_n, x) - \tilde{V}_i(t_n, x)| \geq \delta) \leq \begin{cases} 2 \exp \left(-\frac{M \left(\frac{M-k}{M} - p_{\delta/(4C_2)}^c \right)_+^2}{2} \right) & \text{if } \delta/C_2 \leq 1, \\ 2 \exp \left(-\frac{M \left(\frac{M-k}{M} - p_{\sqrt{\delta}/(4C_2)}^c \right)_+^2}{2} \right) & \text{if } \delta/C_2 > 1. \end{cases}$$

Where $p_r^c(x) = \mathbb{P}(X_{t_n}^1 \notin B_r(x))$.

Proof. As in the proof of Lemma C.6 we need to estimate $\mathbb{P}(U_n(x) \geq \hat{\delta})$ where $U_n(x) = \max_{s \in \mathcal{N}_{t_n}(x)} \|X_{t_n}^s - x\|$. Proceeding similarly but without the covering argument we get from Hoeffding's inequality that

$$\mathbb{P}(U_n(x) \geq \hat{\delta}) \leq 2 \exp \left(-\frac{M \left(\frac{M-k}{M} - p_{\hat{\delta}}^c \right)_+^2}{2} \right).$$

□

Similarly, Lemma C.8 can be modified to account for the fixed x using the above lemmas. The proof of Theorem 5.4 is then an immediate consequence.

D.1. Proof of Theorem 5.6.

Definition D.3. A random variable X is sub-exponential with parameter $\lambda > 0$ if

$$\mathbb{E}[e^{s(X - \mathbb{E}[X])}] \leq e^{\frac{s^2 \lambda^2}{2}}, \quad (\text{D.1})$$

for all $|s| \leq 1/\lambda$.

We begin by stating the following classical variant of Lemma C.3 from probability theory and is a direct consequence of the definition of sub-exponential random variables and the Chernoff bounding method:

Lemma D.4. Let X_1, \dots, X_n be i.i.d. sub-exponential random variables with parameter $\lambda > 0$, then for any $\delta > 0$ we have for some constant $C > 0$ depending on λ that

$$\mathbb{P}(|\bar{X}_n - \mathbb{E}[\bar{X}_n]| \geq \delta) \leq 2 \max \left\{ e^{-\frac{n\delta^2}{2\lambda^2}}, e^{-\frac{n\delta}{2\lambda}} \right\},$$

where $\bar{X}_n = \frac{1}{n} \sum_{i=1}^n X_i$.

Proceeding a similar way as in the proof of Theorem 5.3. We first note that Lemma C.1 still holds as the upper bounds in (5.6) are of the form $K(\|x - y\|)$, and as such the change of variables argument still holds. In the proof of Lemma C.4 we note that the random variables $\varepsilon_{(s,\hat{s})}$ are now sub-exponential with a parameter depending only on λ_1 and L , and as such we can use Lemma D.4 instead of Lemma C.3, which gives us the following bound

$$\mathbb{P} \left(\sup_x |\widehat{V}_i(t_n, x) - \widetilde{V}_i(t_n, x)| \geq \delta \mid D_T \right) \leq 2 \binom{M}{k} \max \left\{ e^{-\frac{km_Y \delta^2}{2\sigma^2}}, e^{-\frac{km_Y \delta}{2\sigma}} \right\}.$$

Lemmas C.5 and C.8 follows in the same way as before and the proof of Theorem 5.6 follows in the same way as the proof of Theorem 5.3.

APPENDIX E. JUMP DIFFUSION PROCESSES AND VERIFICATION OF (5.6)

In this section we will verify (5.6) for the following 1d-jump diffusion process

$$X_t = x + \int_0^t b(X_s) ds + \int_0^t \sigma(X_s) dW_s + \sum_{i=1}^{\infty} Y_i \mathbf{1}_{\{T_i \leq t\}}, \quad (\text{E.1})$$

where $b, \sigma : \mathbb{R} \rightarrow \mathbb{R}$ are Lipschitz continuous functions, W_t is a standard Brownian motion, Y_i are i.i.d. random variables which have mean zero and finite moments of all orders with density φ . The jump times T_i are the arrival times of a Poisson process $\{N_t\}$ with intensity $\lambda > 0$.

Define the convolution density

$$q_t(x, y) = \int_{\mathbb{R}} \varphi(y - z) p_t(x, z) dz,$$

where $p_t(x, y)$ is the transition density of the diffusion part of the process, specifically $p_t(x, y)$ is the transition density for

$$Z_t = x + \int_0^t b(Z_s) ds + \int_0^t \sigma(Z_s) dW_s.$$

Proposition E.1 ([KHNT22]). For any $t > 0$ and any $x, y \in \mathbb{R}$, the transition density $f_t(x, y)$ of X_t given $X_0 = x$, is given by the following convolution

$$\begin{aligned} f_t(x, y) &= p_t(x, y) e^{-\lambda t} \\ &+ \sum_{n=1}^{\infty} \int_{0 < t_1 < \dots < t_n < t < t_{n+1}} q_{t_1-t_0} \star \dots \star q_{t_n-t_{n-1}} \star p_{t-t_n} \lambda^{n+1} e^{-\lambda t_{n+1}} dt_1 \dots dt_{n+1}, \end{aligned}$$

where

$$(g_1 \star g_2)(x, y) = \int_{\mathbb{R}} g_1(x, z) g_2(z, y) dz.$$

From the above proposition we note that the derivative of the transition density with respect to x will then be given by

$$\begin{aligned} \partial_x f_t(x, y) &= \partial_x p_t(x, y) e^{-\lambda t} \\ &+ \sum_{n=1}^{\infty} \int_{0 < t_1 < \dots < t_n < t < t_{n+1}} \partial_x q_{t_1-t_0} \star \dots \star q_{t_n-t_{n-1}} \star p_{t-t_n} \lambda^{n+1} e^{-\lambda t_{n+1}} dt_1 \dots dt_{n+1}, \end{aligned}$$

where

$$\partial_x q_{t_1-t_0} = \int_{\mathbb{R}} \varphi(y - z) \partial_x p_{t_1-t_0}(x, z) dz.$$

If we assume the same gradient bounds for p_t as we did earlier in (5.2) which is in fact a Gaussian upper bound. We can use the same arguments as in the proof of the upper density bound as in [KHNT22] to get the following result.

Proposition E.2. *Assume that φ is sub-exponential, then for any $t > 0$ and any $x, y \in \mathbb{R}$, the derivative of the transition density $f_t(x, y)$ of X_t given $X_0 = x$, with respect to x is given by*

$$|\partial_x f_t(x, y)| \leq \frac{C}{\sqrt{t}} e^{-C|x-y|}.$$

As such we have that the transition density satisfies the bounds in (5.6) for any $x, y \in \mathbb{R}$ and $t > 0$.

Email address: martin.andersson@math.uu.se

MARTIN ANDERSSON, DEPARTMENT OF MATHEMATICS, UPPSALA UNIVERSITY, S-751 06 UPPSALA, SWEDEN

Email address: benny.avelin@math.uu.se

BENNY AVELIN, DEPARTMENT OF MATHEMATICS, UPPSALA UNIVERSITY, S-751 06 UPPSALA, SWEDEN

Email address: bakkenolofsson@gmail.com

MARCUS OLOFSSON, DEPARTMENT OF MATHEMATICS, UPPSALA UNIVERSITY, S-751 06 UPPSALA, SWEDEN